Published online 14 July 2021

Nucleic Acids Research, 2021, Vol. 49, No. 14 ***8037–8059***
https://doi.org/10.1093/nar/gkab607

HBO1 is a versatile histone acyltransferase critical for promoter histone acylations

Yanhui Xiao[1,2,†], Wenjing Li[3,†], Hui Yang[4,†], Lulu Pan[5], Liwei Zhang[6], Lu Lu[1], Jiwei Chen[1], Wei Wei[1], Jie Ye[3], Jiwen Li[1], Guohong Li[6], Yong Zhang[4], Minjia Tan[5], Jianping Ding[3,*] and Jiemin Wong[1,2,*]

[1]Shanghai Key Laboratory of Regulatory Biology, Institute of Biomedical Sciences and School of Life Sciences, East China Normal University, Shanghai 200241, China, [2]Joint Center for Translational Medicine, School of Life Sciences, East China Normal University and Fengxian District Central Hospital, Shanghai 201499, China, [3]State Key Laboratory of Molecular Biology, Shanghai Institute of Biochemistry and Cell Biology, Center for Excellence in Molecular Cell Science, Chinese Academy of Sciences; University of Chinese Academy of Sciences, Shanghai 200031, China, [4]Translational Medical Center for Stem Cell Therapy & Institute for Regenerative Medicine, Shanghai East Hospital, School of Life Science and Technology, Shanghai Key Laboratory of Signaling and Disease Research, Tongji University, Shanghai 200092, China, [5]State Key Laboratory of Drug Research, Shanghai Institute of Materia Medica, Chinese Academy of Sciences, Shanghai 201203, China and [6]National Laboratory of Biomacromolecules, CAS Center for Excellence in Biomacromolecules, Institute of Biophysics, Chinese Academy of Sciences, Beijing, China

Received June 12, 2021; Editorial Decision June 26, 2021; Accepted July 12, 2021

ABSTRACT

Recent studies demonstrate that histones are subjected to a series of short-chain fatty acid modifications that is known as histone acylations. However, the enzymes responsible for histone acylations *in vivo* are not well characterized. Here, we report that HBO1 is a versatile histone acyltransferase that catalyzes not only histone acetylation but also propionylation, butyrylation and crotonylation both *in vivo* and *in vitro* and does so in a JADE or BRPF family scaffold protein-dependent manner. We show that the minimal HBO1/BRPF2 complex can accommodate acetyl-CoA, propionyl-CoA, butyryl-CoA and crotonyl-CoA. Comparison of CBP and HBO1 reveals that they catalyze histone acylations at overlapping as well as distinct sites, with HBO1 being the key enzyme for H3K14 acylations. Genome-wide chromatin immunoprecipitation assay demonstrates that HBO1 is highly enriched at and contributes to bulk histone acylations on the transcriptional start sites of active transcribed genes. HBO1 promoter intensity highly correlates with the level of promoter histone acylation, but has no significant correlation with level of transcription. We also show that HBO1 is associated with a subset of DNA replication origins. Collectively our study establishes HBO1 as a versatile histone acyltransferase that links histone acylations to promoter acylations and selection of DNA replication origins.

INTRODUCTION

In eukaryotic cells, DNA wraps around histone octamers to form nucleosomes, the basic units of chromatin. Post-translational modification of protruding histone tails is a major mechanism for regulation of chromatin structure and function and has been shown to play critical roles in all DNA templated processes including transcription, DNA damage repair, and DNA replication (1–4). Histone acetylation, one of the best-characterized dynamic histone modifications, is catalyzed by lysine acetyltransferases (KATs) and removed by deacetylases (HDACs) (5–7). KATs catalyze acetylation on histones and non-histone proteins via transferring the acetyl group from acetyl-CoA to the ε-amino group of lysine residues. On the basis of structural similarity and sequence conservation within their catalytic domains, KATs have been divided into several main families including p300/CBP, the GNAT family GCN5 and PCAF, and the MYST family Tip60, MOZ, MORF, HBO1 and hMOF (also known as KAT5, KAT6A, KAT6B, KAT7 and KAT8, respectively) (5,8,9). Accumulative studies indicate that histone acetylation is associated with transcriptional activation process and at least two mechanisms have been proposed to account for its effect on transcription. Acetylation can neutralize the positive charge on lysine residues, which

*To whom correspondence should be addressed. Tel: +86 21 54345013; Fax: +86 21 54344922; Email: jmweng@bio.ecnu.edu.cn
Correspondence may also be addressed to Jianping Ding. Email: jpding@sibcb.ac.cn
†The authors wish it to be known that, in their opinion, the first three authors should be regarded as Joint First Authors.

reduces the interaction of histone tails with DNA and facilitates chromatin accessibility. In addition, lysine acetylation also provides binding sites for transcriptional regulatory proteins that often contain bromodomains (2,10,11).

Recent studies indicate that, in addition to acetylation, histone lysine residues are also modified by chemically diverse acyl molecules, resulting in histone propionylation, butyrylation, crotonylation, malonylation, succinylation etc (12–18). Like acetylation, these diverse acyl modifications depend on their respective charged acyl-CoAs, which are also intermediate metabolites of cellular metabolism (12). The findings of these novel types of acylations further strengthen the molecular links between cellular metabolism and epigenetic modifications, suggesting that cellular metabolic state can potentially directly controls gene expression via various types of histone acylations (12,18,19). These findings also raise critical questions as to what enzymes are involved in various types of histone acylations. Furthermore, as these acylations vary in size, hydrophobicity and charge of their acyl moiety, they are likely to differentially impact chromatin structure and function, as revealed by recent studies on histone crotonylation (12,18). So far various KAT enzymes have been shown to catalyze lysine acylations to various extent *in vitro* and *in vivo*. For example, p300 and CBP have been shown to catalyze nearly all types of reported acylations including the propionylation, butyrylation, 2-hydroxylisobutyrylation, β-hydroxybutyrylation, crotonylation and succinylation (12,13,20–22). On the other hand, the GNAT family KATs GCN5 and PCAF have been shown to catalyze efficiently propionylation, but poorly active for butyrylation and crotonylation (23,24). Structural analysis revealed that the active site of p300 can accommodate various acyl-CoAs, although a substrate engagement-induced conformational remodeling is needed to accommodate the aliphatic portion of acyl-CoA into a hydrophobic pocket in the enzyme's active site (22). The lack of such a pocket in GCN5 also explains why they can catalyze propionylation but not butyrylation and crotonylation (24).

As a member of the MYST family KATs, the histone acetyltransferase HBO1 was first identified as a DNA replication initiator subunit ORC1-interacting protein via yeast two-hybrid assay (25). HBO1 is a major source of histone H3 and H4 acetylation and play critical roles in transcription and regulation of DNA replication (26–31). HBO1 is required for mouse embryonic development and loss of HBO1 results in profound reduction of histone H3 acetylation at K14 (28). Biochemical studies revealed that HBO1 exists in two distinct types of multisubunit complex consisting of ING4/5, hEaf6, and either scaffold proteins JADE1/2/3 or BRPF1/2/3 (26,32–34). The ING4/5 subunit enables HBO1 activity towards chromatin substrates with H3K4me3-bearing nucleosomes (33,34). Although both types of scaffolds confer HBO1 the activity to acetylate both H3 and H4 in core histones, they display distinct specificities in chromatin, as the JADE1/2/3-containing HBO1 complexes preferentially acetylate histone H4 and the BRPF1/2/3-containing complexes acetylate histone H3 in nucleosomes (35). Recently we identified a short N-terminal region of BRPF2 that is sufficient to interact with and substantially stimulate HBO1 activity to acetylate H3K14 (36). Among the MYST family KATs, MOF has been reported for both histone propionylation and crotonylation activities (21,37), and MOZ (KAT6A) and MORF (KAT6B) for histone propionylation activity (38). However, as a major activity for cellular histone H3 and H4 acetylation in cells, HBO1 has not been systematically characterized for histone acyltransferase activity, although it was shown to catalyze histone propionylation in vitro (37).

Here, we report that HBO1 is a versatile histone acyltransferase that catalyzes not only histone acetylation but also propionylation, butyrylation and crotonylation both *in vivo* and *in vitro*. We provide structural evidence that the minimal HBO1/BRPF2 complex can accommodate not only acetyl-coA, but also propionyl-coA, butyryl-coA and crotonyl-coA. We show that HBO1 is highly enriched at and required for bulk histone acylations at promoters. We also show that HBO1 is associated with a subset of early replicating DNA replication origins. Finally, we provide evidence that histone propionylation could play important roles in HBO1-mediated transcriptional regulation.

MATERIALS AND METHODS

Cell culture

HeLa and 293T cells were cultured in DMEM (GIBCO) with 10% fetal bovine serum (FBS) (Intergen). HCT116 cells were cultured in McCoy's 5A (GIBCO) with 10% FBS. mESCs (CGR8) were cultured on 0.1% gelatin-coated plates in GMEM ESC medium (GIBCO) containing 15% FBS (GIBCO), 2 mM L-glutamine (Hyclone), 100 mM nonessential amino acids (Hyclone), 0.1 mM 2-mercaptoethanol (GIBCO), 1 mM sodium pyruvate and leukemia inhibitory factor (LIF, 1 000 U/ml, Chemicon).

Antibodies and reagents

For antibodies and reagents used in this study, please see Supplementary Table S1.

Plasmids

Expression plasmids used in this study include FLAG-JADE1, FLAG-JADE2, FLAG-JADE3, FLAG-HBO1, FLAG-HBO1(E508Q), MYC-HBO1, FLAG-HA-CBP, MYC-p300, FLAG-MOF, FLAG-TIP60, HA-ING5 and HA-EAF6 in pCDNA3.1 vector; FLAG-BRPF2 and HA-BRPF2 in pCDNA3.0 vector; and pEGFP-C1-BRPF2. The plasmids for knockdown include pLKO.1-puro-shHBO1 (human/mouse), pLKO.1-puro-shJADE1, and pLKO.1-puro-shBRPF2. Plasmid for knockout of HBO1 in HeLa cells was pLKO.1-puro-HBO1sgRNA. Construction of HBO1-KO HeLa cell lines by CRISPR/Cas9 technology was essentially as described (39), with the following guide RNAs:

HBO1 sgRNA1: GGGTGACTCGAGCAGATCGT
HBO1 sgRNA2: CCTGACAAGCGAGTATGACT

Both sgRNAs worked efficiently and the HBO1-KO cell lines were isolated from knockout with sgRNA1.

HBO1-BRPF2 complex expression and purification

The HBO1-BRPF2 complex was expressed and purified as previously described (36). Briefly, the pET-28a plasmid containing the cDNA encoding the catalytic domain of HBO1 and the pET-22b plasmid containing the cDNA encoding the N-terminal region of BRPF2 (residues 31–80) were co-transformed into *E. coli* BL21 (DE3) Codon-Plus strain. The transformed cells were grown at 37 ^{o}C to an absorbance of 0.8 at OD_{600} and induced with 0.2 mM IPTG at 16^{o}C for 24 h. The HBO1-BRPF2 complex was purified by affinity chromatography via the N-terminal His_6 tag of BRPF2 and cleaved from the tag with tobacco etch virus protease. Then the complex was further purified using a Ni-NTA column and a Superdex 200 16/600 column (GE Healthcare).

Crystallization, data collection and structure determination

Crystals of HBO1-BRPF2 complex in apo form and in different ligand-bound form were obtained as previously described (36). Briefly, to obtain different ligand-bound complexes, the HBO1-BRPF2 complex was mixed with propionyl-CoA, butyryl-CoA, crotonyl-CoA and succinyl-CoA (Sigma) at a molar ratio of 1:4 prior to crystallization. Crystals of HBO1-BRPF2 complex in apo form were grown in drops consisting of the protein solution and the reservoir solution (0.1 M MES, pH 6.5, 12% w/v PEG 20 000). Crystals of HBO1-BRPF2 in complex with propionyl-CoA were grown in drops consisting of the protein solution and the reservoir solution (0.1 M HEPES, pH 7.5, 12% w/v PEG 3350). Crystals of HBO1-BRPF2 in complex with butyryl-CoA were grown in drops consisting of the protein solution and the reservoir solution (0.1 M Tris, pH 8.5, 20% w/v PEG 6000). Crystals of HBO1-BRPF2 in complex with crotonyl-CoA were grown in drops consisting of the protein solution and the reservoir solution (0.03 M Citric acid, 0.07 M BIS-TRIS propane, pH 7.6, 20% w/v PEG 3,350). Crystals of HBO1-BRPF2 in complex with succinyl-CoA were grown in drops consisting of the protein solution and the reservoir solution (0.2 M L-Proline, 0.1 M HEPES, pH 7.5, 24% w/v PEG 1500). The crystals were cryoprotected using the reservoir solution supplemented with 30% glycerol and then flash-cooled into liquid N_2. Diffraction data were collected at BL17U1 of Shanghai Synchrotron Radiation Facility and BL19U1 of National Facility for Protein Science Shanghai, and processed with HKL2000 or HKL3000 (40). The statistics of the diffraction data are summarized in Table 2. All of the crystal structures were solved by the molecular replacement (MR) method using the HBO1-BRPF2 complex (PDB code 5GK9) structure as the search model. Model building was performed with Coot (41) and structure refinement was carried out using Refmac5 (42) and Phenix (43). Structural analysis was carried out using programs in CCP4 (44). The structure figures were generated using Pymol (www.pymol.org) (45). The statistics of the structure refinement and the quality of the final structure models are also summarized in Table 2.

Surface plasmon resonance (SPR) binding assays

The purified HBO1-BRPF2 complex was first diluted with 10 mM sodium acetate (pH 5.5) to the concentration of 150 μg/ml. Then the protein complex was injected at a constant flow rate of 10 μl/min for 900 s and immobilized to CM5 sensor chips (GE Healthcare) using the amine coupling kit, which resulting in the level of protein immobilization is about 20 kRU. All SPR measurements were performed at 25°C using Biacore 8K instrument (GE Healthcare) in running buffer containing 10 mM HEPES (pH7.4) and 150 mM NaCl at a flow rate of 30 μl/min. To determine the binding affinities, CoA or different acyl-CoAs were analyzed using concentration response experiments. Specifically, CoA or different acyl-CoAs (10 μM) were 2-fold serially diluted in the running buffer. The resulting increasing concentrations of the ligands were injected over HBO1–BRPF2 complex in the running buffer for 240 s. The surface was washed between each binding cycle with running buffer for 270 s and the ligand was fully dissociated. The experimental data were analyzed by fitting to both of a 1:1 steady-state affinity model and a kinetic binding model to determine the K_D, k_a and k_d values of different ligands in the Biacore 8K evaluation software.

Knockdown with shRNA

Mission shRNAs were cloned into pLKO.1-PURO vector, then were co-transfected with psPAX2 and pMD2G into HEK293T cells for packaging of lentivirus. The resulting lentiviruses were used to infect cells of interest. 36 hours after infection, puromycin was added to the culture at a final concentration of 2 μg/ml, and 4 days after infection the cells were collected for analyses by WB for protein levels and/or qPCR for RNA levels. The shRNA sequences for HBO1, JADE1 and BRPF2 were listed in Supplementary Table S2.

Western blot (WB) analysis and immunofluorescence staining (IF)

For WB analysis, cells were lysed directly in 1× loading buffer. Proteins were separated with 10% or 12% SDS-PAGE gels and WB was performed essentially as described (21). IF staining was performed essentially as described (46). All WB and IF data were repeated at least twice.

Preparation of core histones for *in vitro* acylation assays from HeLa cells

Preparation of core histones was performed as described (47).

Immunoaffinity purification of HBO1 and complexes from HEK293T cells

To purify HBO1 or its complexes with JADE1/2/3 or BRPF2 scaffold proteins, plasmid encoding FLAG-HBO1 was transfected into two 10 cm dish HEK293T cells along or together with plasmids encoding one of FLAG-tagged scaffold proteins. As little activity was observed when FLAG-HBO1 or FLAG-scaffold was expressed in HEK293T alone, expression of both FLAG tagged HBO1 and scaffold allowed more efficient purification of the HBO1/scaffold complexes. Two days after transfection, cells were collected, washed with ice PBS, and then lysed

with three volume of lysis buffer (50 mM Tris–HCl pH7.5, 150 mM NaCl, 1% triton X-100, 1 mM EDTA, 1 mM DTT, 8% glycerinum plus protease inhibitors) on ice for 30 min. After centrifugation at 12 000 rpm, 4°C for 20 min, the supernatants were collected and diluted with 2/3 volume of binding buffer (20 mM Tris–HCl pH7.5, 150 mM NaCl, 1 mM EDTA, 8% glycerinum plus protease inhibitors) and incubated with 25 μl pre-washed M2 beads at 4°C with rotation for at least 4 h. After a short spin, the M2 beads were washed three times with washing buffer (20 mM Tris–HCl pH7.5, 150 mM NaCl, 0.1% Triton X-100, 1 mM EDTA, 1 mM DTT, 8% glycerinum plus protease inhibitors). After centrifugation at 4°C, 3000 rpm for 3 min, the supernatants were discarded and beads were incubated with 150 μl elution buffer (20mM Tris-HCl pH7.5, 150 mM NaCl, 0.1% NP40, 1 mM DTT, 10% glycerinum plus protease inhibitors, and 200 μg/ml FALG peptide) and rotated at 4°C overnight. The supernatants containing FLAG-HBO1 or complexes were collected after a short spin and aliquoted for storage at –80°C freezer or used for *in vitro* acylation assay directly.

In vitro histone acylation assay

In vitro histone assays were carried out at 37°C for 1 h in Buffer A (25 mM Tris–HCl pH 8.0, 150 mM NaCl, 10% glycerinum, 2 mM $MgCl_2$, 1 mM sodium butyrate, 1 mM DTT) with 100 μM acetyl-CoA, propionyl-CoA, butyryl-CoA or crotonyl-CoA and 1 μg core histones, recombinant histone octamer or recombinant nucleosomes purchased from Active Motif. The reactions were stopped by 3× SDS, and histone acylations were detected by WB analysis using various antibodies as indicated. Alternatively, histone acylations were analyzed by mass spectrometry as described (48).

SILAC assay for histone acylations

To quantitatively determine the effect of knockdown of HBO1 on histone acylations by SILAC (stable isotopic labeling of amino acids in cell culture), Hela cells were grown in lysine and arginine-free DMEM supplemented with 10% dialyzed FBS, L-Arginine(84ug/ml) and L-lysine (146 ug/ml) or L-arginine $^{13}C_6$ hydrochloride (84 ug/ml) and L-lysine-4,4,5,5-d_4 hydrochloride (146ug/ml), respectively. Cells were grown for more than seven generations to achieve more than 98% labeling efficiency. Then L-arginine $^{13}C_6$ hydrochloride and L-lysine-4,4,5,5-d_4 hydrochloride labeled cells were infected with lentiviral shHBO1 to knock down HBO1, whereas L-arginine and L-lysine labeled cells were infected with lentiviral shVec. Four days after infection, the same quantity of shVec and shHBO1 treated cells were collected and mixed before processed for histone preparation for MS spectrometry analysis (48).

RNA extraction and RT-qPCR

For RNA-seq analysis of global gene expression, equivalent numbers of cells from each group were used for preparation of RNAs. The same amount of spike-in yeast RNAs (10%) was added to each RNA sample. RNA was extracted from cells using total RNA extraction reagent (Toroivd, code NO. A211-01 or Toyobo company) by following the manufacturer's protocol.

For RT-qPCR analysis, 2 μg total RNA were reverse-transcribed with TransScriptR One-Step gDNA Removal and cDNA Synthesis SuperMix (TransGen Biotech Co., Ltd). Gene expression levels were determined using qPCR with the CFX96 RealTime System (Bio-Rad) using TransStart Green qPCR SuperMix (TransGen Biotech Co., Ltd) and normalized to GAPDH or β-actin expression. All RT-qPCR data are represented as the mean fold change in relative expression of three independent experiments ± SD (Primers for RT-PCR are listed in Supplementary Table S2).

Chromatin immunoprecipitation (ChIP) and ChIP-sequencing (ChIP-seq)

ChIP assays were performed as previously described (49).

For ChIP-seq analysis, a total amount of 50 ng DNA per sample was used as input material for library construction. Sequencing libraries were generated using NEBNext® Ultra™DNA Library Prep Kit from Illumina® (NEB,USA) by following manufacturer's recommendations and index codes were added to attribute sequences to each sample. The clustering of the index-coded samples was performed on a cBot Cluster Generation System using HiSeq Rapid Duo cBot Sample Loading Kit (Illumia) according to the manufacturer's instructions. After cluster generation, the library preparations were sequenced on an Illumina Hiseq 2500 platform and 150 bp pair-end reads were generated. All ChIP-seq experiments were carried out with three independent biological samples.

ChIP-seq and RNA-seq data processing and normalization

The ChIP-seq reads were aligned to the human genome build hg38 and mouse genome build mm9 using the bowtie2 (v2.3.5.1) (50) with the default parameters. The human ChIP-seq reads were divided by total *Mus musculus* mapped reads to get quantitative information in the form of reference-adjusted reads per million (RRPM) as described in Orlando *et al.* (51) and then signal tracks for each sample were generated using MACS2 (v2.1.3) pileup function (52) and visualized in UCSC genome browser (53). To examine the reproducibility of the ChIP-seq experiments, we calculated the correlation of RRPM between biological replicates in 1-kb genome bins. We then pooled the two most correlated biological replicates (see Supplementary Figure S7) for each ChIP-seq together from reads and further aligned and normalized. The ChIP-seq peaks of HBO1 in control HeLa cells were called by MACS2 (v2.1.3) with the parameters –nomodel –broad –shift = 73 -q 0.001, and further filtered to require at least 3-fold enrichment over the chromatin input DNA. The ChIP-seq data can be seen at http://genome.ucsc.edu/cgi-bin/hgTracks?db=hg38&hubUrl=http://119.3.41.228/wong_chip_bw/Wong_Hub/hub.txt.

For RNA-seq analysis of gene expression profiling, three biological replicates were analyzed for each sample. The resulting RNA-seq data were analyzed for Pearson's correlation coefficients and shown to have an excellent

consistency (see Supplementary Figure S8). The RNA-seq reads were aligned to the human genome build hg38 and yeast genome build sacCer3 using HISAT2 (v 2.1.0) (54) with the default parameters. The expression levels for all RefSeq genes were quantified to fragments per kilobase million (FPKM) using StringTie(v2.1.2) (55), and FPKM values of replicates for each condition were highly correlated then were averaged. Transcript-level read counts for each sample were calculated with the program prepDE.py (http://ccb.jhu.edu/software/stringtie/dl/prepDE.py), and then differentially expressed genes were called using edgeR (v 3.26.7) (56) with fold change cutoff $\geq$1.5 and *P*-value $<$0.05.

The raw sequence data reported in this paper have been deposited in the Genome Sequence Archive (57) in National Genomics Data Center (58), Beijing Institute of Genomics, Chinese Academy of Sciences, under accession number HRA000828 that are publicly accessible at http://bigd.big.ac.cn/gsa-human.

For ChIP-qPCR, the primers are designed according to the peak at gene promoter region, and Data are represented as mean of % input ± SD of three biological repeats, the primers a listed in Supplementary Table S2.

Peak calling and selection of DNA replication origin sites

H4K20me2, ORC1, NS and BrdU were downloaded and reanalyzed as previously described. First, raw data was cleaned with the 'Q30' threshold using FASTX-Tools (http://hannonlab.cshl.edu/fastx_toolkit/). Then, clean tags were mapped to human genomic assembly (version GRCh38) using bowtie2 (version 2.2.5) with default parameters (50). Tags mapped to chromosome Y or mitochondrial chromosome were removed. Unique Tags with high mapping qualities were filtered using samtools (-q 15) (59).

ChIP-seq and NS-seq peaks were called using MACS (version 1.4.2, *P*-value $\leq 1e^{-5}$) (52) and PeakSeq (version 1.3.1, false discovery rate $\leq$ 0.005) (60) against their corresponding native genomic input with a shift size of 75 bp (*P*-value $\leq 1e^{-5}$). During the procedure of NS-seq, RNAase treatment was parallelly used to removes the RNA primer of nascent strand, resulting in digestion of the nascent strand by lambda-exonuclease. Thus, NS peaks with significant decays in the corresponding RNase treated sample were removed (fold change $\leq -\log_2(1.5)$. Fisher's exact test, FDR $\leq$ 0.05). Peaks within 500 bp were further merged using BEDTools (version 2.17.0) (61). Genome-wide profiles for ChIP-seq and NS-seq were generated in wiggle format using those shifted alignments and further normalized using RPM algorithm.

H4K20me2, ORC1 and NS peaks (H4K20me2, ORC1) or NS regions within 5 kb were defined to have interactive relationships between each other. NS peaks overlapped with both H4K20me2 and ORC1 were defined as true DNA replication origins and used for further analysis. The analysis of DNA replication timing was as described (62).

Bioinformatic data visualization

Heatmap of tag densities around centers of various enriched regions were summarized using deepTools (version 2.3.5) (63) and visualized in R. Genome-wide tracks of high-throughput data about DNA replication were visualized in the IGV (integrative genomics viewer) browser (version 2.6.0) (53).

Statistical analyses

The statistical significance was analyzed by Student's *t* test. $P < 0.05$(*), $P < 0.01$ (**) and $P < 0.001$ (***) indicate statistically significant changes.

RESULTS

The scaffold/HBO1 complexes catalyze multiple types of histone acylations *in vitro*

We have recently shown that a short N-terminal region (residues 31–80) of BRPF2 is sufficient to bind to the HBO1 MYST domain and stimulate its HAT activity (36). To test if HBO1 catalyzes histone acylations other than acetylation, we therefore expressed in bacteria and purified the complex composed of the short N-terminal BRPF2 and the HBO1 MYST domain, that we named nBRPF2–HBO1 hereafter. We then carried out *in vitro* acylation assays using core histone substrates prepared from glucose and serum starved HeLa cells and individual respective acyl-CoA as donors and examined histone acylations by Western blotting (WB) using antibodies specific for each type of pan acyl-lysine (Supplementary Figure S1). The representative results, as shown in Figure 1A, demonstrated that the nBRPF2–HBO1 complex is able to catalyze not only histone acetylation, as expected, but also propionylation, butyrylation and crotonylation. Consistent with previous reports with core histone substrates and the complete HBO1 complexes (35), we found that the nBRPF2–HBO1 complex catalyzed acetylation on both H3 and H4. Similarly, we observed that the nBRPF2–HBO1 complex also efficiently catalyzed propionylation, butyrylation and crotonylation on both H3 and H4. These results indicate that the BRPF-containing HBO1 complex is likely a versatile histone acyltransferase.

We next tested whether the JADE1/2/3-containing HBO1 complexes are also capable of catalyzing multiple types of histone acylations. To this end, we expressed FLAG-HBO1 alone or co-expressed FLAG-HBO1 together with either FLAG-JADE1, FLAG-JADE2 or FLAG-JADE3 in HEK293T cells. We then prepared the resulting FLAG-HBO1 and FLAG-HBO1 complexes containing FLAG-JADE1, JADE2 or JADE3 through immunoaffinity purification by using anti-FLAG M2 agarose beads. The subsequent *in vitro* acylation assays demonstrated that, while FLAG-HBO1 alone displayed only a weak activity for histone acetylation and propionylation, the presence of JADE1 or JADE2 strongly enhanced its ability to catalyze histone acetylation, propionylation, butyrylation and crotonylation (Figure 1B). JADE3 also promoted HBO1 acyltransferase activity, but to a much less extent, in part possibly due to its weak expression. To ensure the observed acyltransferase activity is intrinsic to HBO1, we prepared the JADE1–HBO1 complexes that contained either wild-type or a mutant HBO1 that contains a 508 glutamic acid to glutamine (E508Q) mutation that reported to

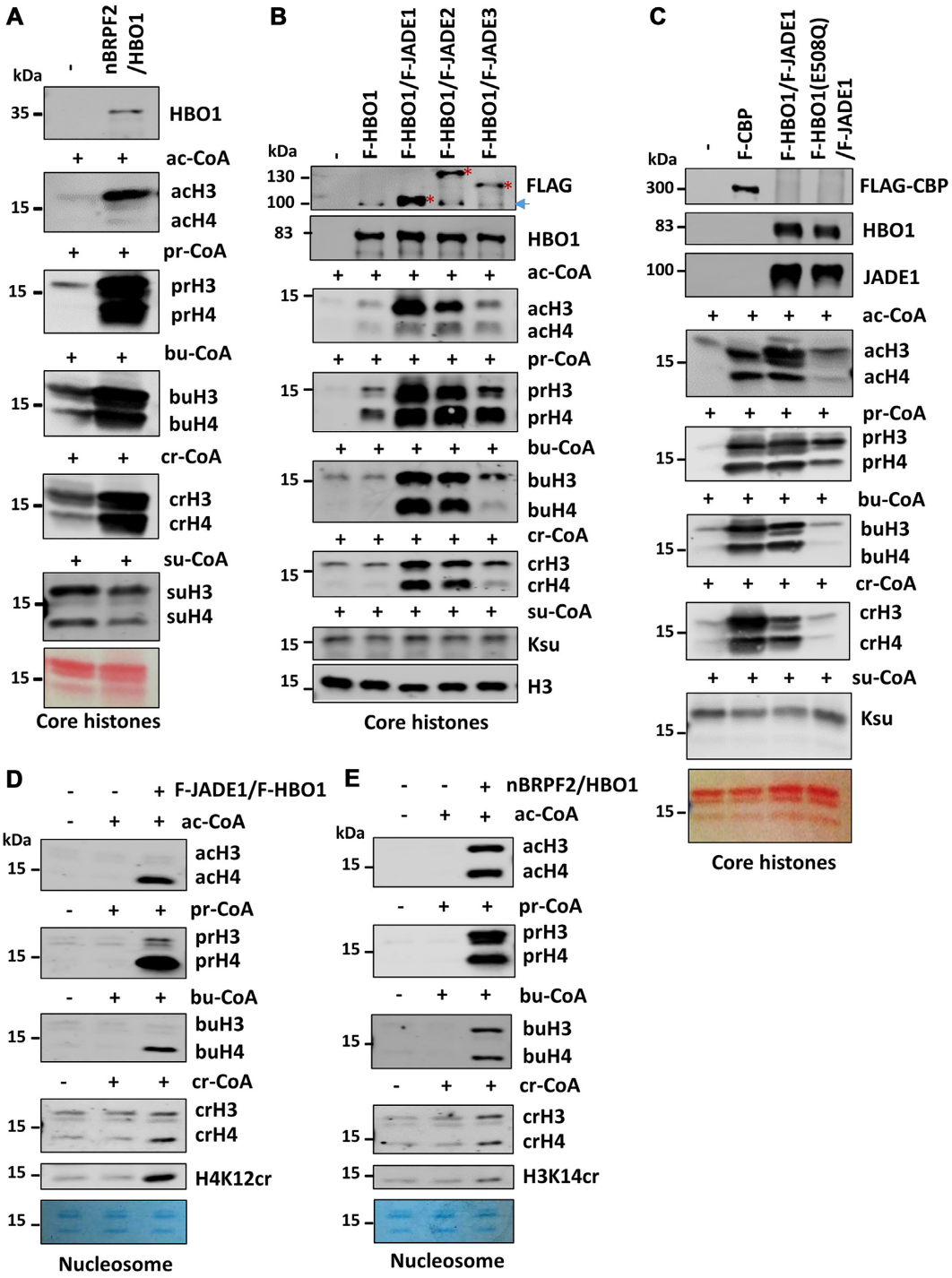

Figure 1. In vitro histone acylations by the JADE1–HBO1 and nBRPF2–HBO1 complexes. (**A**) The nBRPF2–HBO1 complex was purified from E.coli and applied to *in vitro* reactions with core histone substrates and individual acyl-CoAs as indicated. The resulting histones were analyzed for acylations using specific pan acyl-lysine antibodies as indicated. Note nBRPF2–HBO1 was able to catalyze histone acetylation, propionylation, butyrylation and crotonylation. (**B**) The JADE family proteins were co-expressed with HBO1 in HEK293T cells respectively and the resulting JADE/HBO1 complexes were immunoaffinity purified by using anti-FLAG M2 beads and used for *in vitro* histone acylation assay as in (A). (**C**) CBP, JADE1–HBO1 and JADE1–HBO1(E508Q) complexes were expressed and purified from HEK293T cells by immunoaffinity purification and applied to *in vitro* histone acylation assay. (**D**) *In vitro* histone acylation assays were performed with recombinant nucleosome substrate and the JADE1–HBO1 complex. (**E**) *In vitro* histone acylation assays were performed with recombinant nucleosome substrate and the nBRPF2–HBO1 complex.

abrogate the HBO1 KAT activity (64). As CBP is well recognized as a versatile histone acyltransferase (12), we also compared the JADE1–HBO1 complex with CBP in our *in vitro* assay. We found that the JADE1–HBO1(E508Q) complex was severely impaired for nearly all acyltransferase activities as compared to the wild-type JADE1–HBO1 (Figure 1C), indicating that the observed acyltransferase activities are intrinsic to HBO1. This result also excluded the possibility that the observed robust acyltransferase activity for HBO1/JADE1 complex in Figure 1B is solely due to the presence of JADE1 and independent of HBO1. Comparison with CBP revealed that the JADE1–HBO1 complex displayed a comparable activity as CBP for histone propionylation and butyrylation and a reduced activity for histone crotonylation. Under the same experimental conditions, we failed to detect histone succinylation for both CBP and HBO1 (Figure 1C). The failure to detect succinylation activity is not due to problem of Ksu antibody, as this antibody is capable of detecting histone succinylation resulted from nonenzymatic reaction (Supplementary Figure S2). The same results were observed when recombinant histone octamers were used as substrate (data not shown).

The HBO1 complexes have been shown to display distinct substrate preference in acetylation of core histones vs nucleosomes (32,35). To further characterize the acyltransferase activities of HBO1 complexes, we also carried out *in vitro* acylation assays using recombinant nucleosome substrates. Consistent with previous reports, we found that the JADE1–HBO1 complex preferentially acetylated histone H4 in nucleosomes (Figure 1D) rather than both H3 and H4 in core histone substrates (Figure 1B). Similarly, we found that the JADE1–HBO1 complex also nearly exclusively catalyzed propionylation, butyrylation and crotonylation on histone H4 in nucleosomes, which is further confirmed by WB analysis using an antibody specific for H4K12 crotonylation (Figure 1D). On the other hand, the nBRPF2–HBO1 complex catalyzed acetylation, propionylation, butyrylation and crotonylation on both H3 and H4 of nucleosomes (Figure 1E). Thus, our *in vitro* assays provide evidence that the JADE–HBO1 complexes acylate selectively histone H4 in chromatin, whereas the BRPF-HBO1 complexes acylate both H3 and H4, a pattern consistent with reported histone acetylation specificity for JADE/HBO1 and BRPF2/HBO1 complexes.

Binding affinities of HBO1 towards CoA and different acyl-CoAs

Having demonstrated that various HBO1 complexes possess histone propionylation, butyrylation and crotonylation activities *in vitro*, we next investigated the molecular basis underlying the acyltransferase activity of HBO1. Toward this end, we first measured the binding affinity of the nBRPF2–HBO1 complex towards CoA and different acyl-CoAs by surface plasmon resonance (SPR) binding assay. The results show that while CoA displayed a highest binding affinity at 1.64 μM, all the acyl-CoA variants bound to nBRPF2–HBO1 at a comparable level, with 2.05 μM for acetyl-CoA, 2.22 μM for propionyl-CoA, 2.11 μM for butyryl-CoA, 2.58 μM for succinyl-CoA and 6.56 μM for crotonyl-CoA (Figure 2A). Thus, different acyl-CoAs bind nBRPF2–HBO1 basically in the same magnitude, despite that the nBRPF2–HBO1 complex does not possess succinylation activity. These results suggest that the CoA moiety of the acyl-CoAs plays a major role while the acyl-group plays a relative minor role in binding of HBO1.

To better understand how HBO1 binds various acyl-CoA, we also determined the dissociation rate of CoA and each acyl-CoA with nBRPF2–HBO1. As shown in Figure 2A, the trends of the association and dissociation curves of CoA and succinyl-CoA are apparently different from that of other acyl-CoAs. To determine the association and dissociation rate constants (k_a and k_d), we analyzed the experimental data via fitting to a kinetic binding model. Although the binding affinities of HBO1 towards different ligands are comparable, the association and dissociation rates of CoA and succinyl-CoA are both slower than that of other acyl-CoAs (Table 1). The slower dissociation rate may in part explain why we failed to observe histone succinylation for various HBO1 complexes. These data support our *in vitro* activity assays showing robust histone propionylation, butyrylation and crotonylation activity for the HBO1 complexes.

Crystal structures of HBO1-BRPF2 in complex with acyl-CoA variants

To provide conclusive evidence that the nBRPF2–HBO1 binds majority of the acyl-CoAs (Figure 2A and Table 1), we co-crystallized acyl-CoA variants with the nBRPF2–HBO1 complex. Considering that cofactor acetyl-CoA is a common metabolite exists at a relatively high concentration in bacterial cells and might be co-purified with the nBRPF2–HBO1 complex from *Escherichia coli*., we first crystallized the purified nBRPF2–HBO1 without supplementation of any acyl-CoAs. The resulting crystal structure turned out to be in apo form, indicating that the cofactor-binding pocket of the purified nBRPF2–HBO1 is available for binding of different acyl-CoAs. We then co-crystallized propionyl-, butyryl-, crotonyl- and succinyl-CoA with the nBRPF2–HBO1 complex and all crystal structures were solved by molecular replacement using the nBRPF2–HBO1 structure (PDB code 5GK9). The statistics of data collection and structure refinement for all structures are summarized in Table 2 7D0O, 7D0P, 7D0Q, 7D0R and 7D0S.

The overall structure of nBRPF2–HBO1 in apo form and in complex with the different acyl-CoA ligands is essentially identical to that of the nBRPF2–HBO1-acetyl-CoA complex (36) (RMSD < 0.8 Å) (Figure 2B). The calculated composite omit $2F_o - F_c$ maps clearly confirm the binding of the different acyl-CoA ligands despite that the electron densities of the acyl-group of butyryl-, crotonyl- and succinyl-CoA are relatively incomplete compared to that of the propionyl-group of propionyl-CoA (Figure 2C), suggesting that the acyl-groups of different ligands are relatively flexible. In all of the ligand-bound HBO1 structures, the adenosine ring, the pyrophosphate moiety and the pantetheine arm of CoAs make extensive interaction with the cofactor-binding pocket of HBO1 in the same manner. The CoA moieties can be aligned well while the orientations of the acyl-groups are slightly different in different ligand-bound structures (Figure 2B). Structural analyses show that the terminal acyl-groups are cozily located adjacent to residues

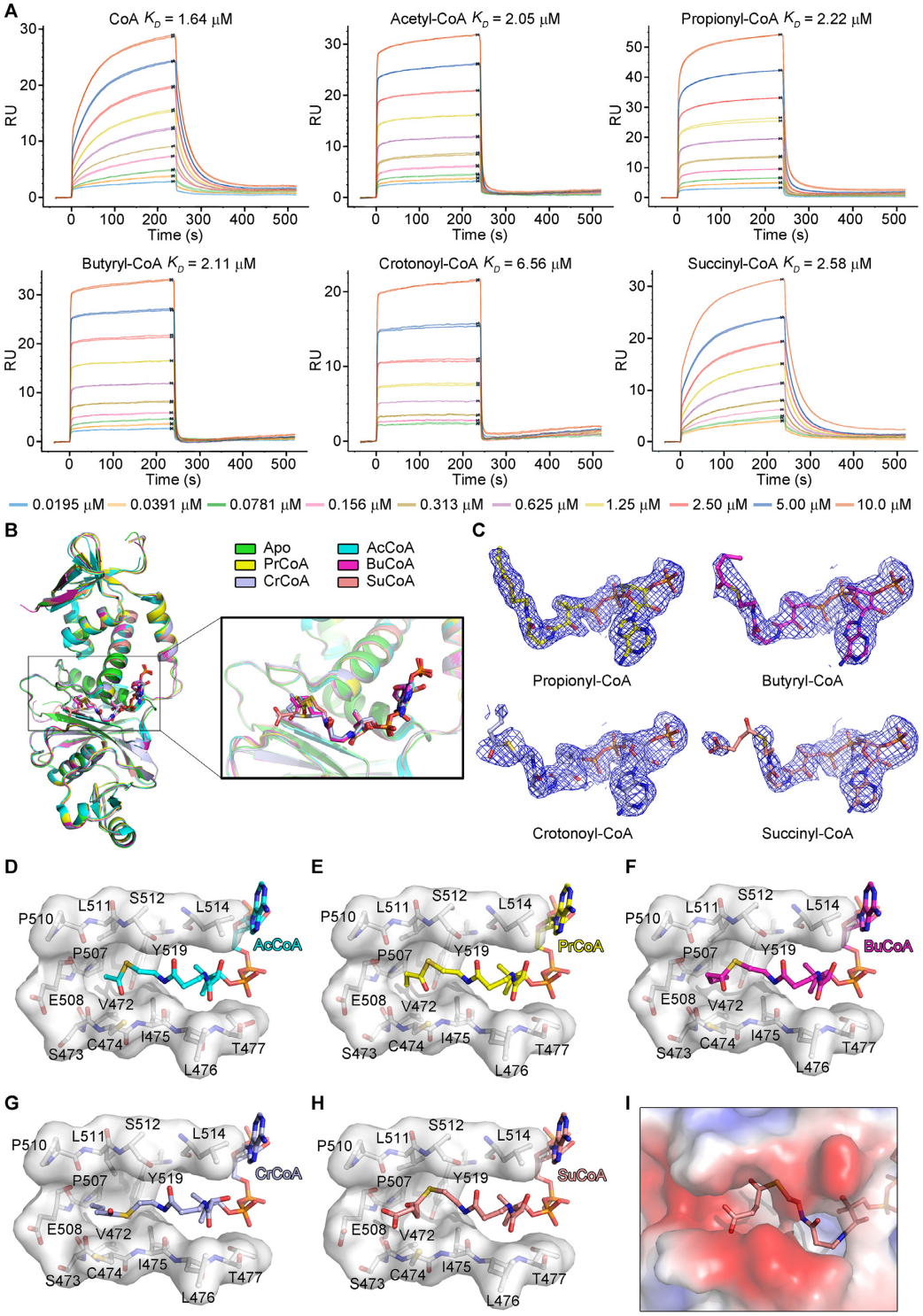

Figure 2. Crystal structures of HBO1-BRPF2 in complex with acyl-CoA variants. (**A**) SPR measurements of the binding affinities of HBO1–BRPF2 towards CoA and different acyl-CoAs. The data were fitted with a 1:1 steady-state affinity model with binding affinity (K_D) indicated. RU, resonance units. (**B**) Comparison of the overall structures of HBO1-BRPF2 in apo form (green), in complex with acetyl-CoA (cyan, PDB code 5GK9), in complex with propionyl-CoA (yellow), in complex with butyryl-CoA (lightmagenta), in complex with crotonyl-CoA (lightblue) and in complex with succinyl-CoA (salmon). The protein complexes are shown in ribbon representation and the bound ligands are shown in ball-and-stick models. (**C**) Representative composite omit *2Fo-Fc* maps (contoured at 0.8 s level, blue) of the bound propionyl-CoA, butyryl-CoA, crotonoyl-CoA and succinyl-CoA in different complex structures. (**D**–**H**) Insertion of (D) the acetyl group of acetyl-CoA, (E) the propionyl group of propionyl-CoA, (F) the butyryl group of butyryl-CoA, (G) the crotonoyl group of crotonyl-CoA and (H) the succinyl group of succinyl-CoA in the acyl-binding pocket of HBO1. The acyl-CoA binding pocket of HBO1 is shown as a transparent white surface. The acyl-CoAs and residues constituting the acyl-CoA binding pocket are shown in ball-and-stick models. **(I)** Electrostatic potential surface of HBO1 surrounding the acyl-binding pocket of HBO1 in the structure of HBO1–BRPF2 in complex with succinyl-CoA. The surface charge distribution is displayed as blue for positive, red for negative and white for neutral.

Table 1. Summary of kinetics and steady state of the interactions between HBO1 and CoA and different acyl-CoAs

	Steady state				Kinetics			
	K_D[a] (μM)	Quality kinetics χ^2 (RU^2)	Affinity χ^2 (RU^2)	R_{max} (RU)	k_a ($M^{-1}s^{-1}$)	k_d (s^{-1})	K_D[b] (μM)	R_{max} (RU)
CoA	1.64	3.47	0.84	28.2	2.23×10^4	2.20×10^{-2}	0.99	25.7
Acetyl-CoA	2.05	1.82	0.43	33.1	1.93×10^5	2.17×10^{-1}	1.13	31.9
Propionyl-CoA	2.22	5.21	3.43	57.6	9.46×10^4	1.21×10^{-1}	1.28	53.4
Butyryl-CoA	2.11	1.50	0.44	35.2	2.26×10^5	2.79×10^{-1}	1.23	34.1
Crotonyl-CoA	6.56	1.02	0.09	31.9	1.06×10^5	3.38×10^{-1}	3.20	26.5
Succinyl-CoA	2.58	3.08	0.78	31.9	1.81×10^4	2.31×10^{-2}	1.27	27.8

k_a, association rate constant; k_d, dissociation rate constant. [a]K_D, steady state affinity; [b]K_D, equilibrium dissociation constant.

Pro507 and Val472, that constitute the base of the acyl-group binding pocket, in the acetyl-, propionyl-, butyryl- and crotonyl-CoA bound structures (Figure 2D–G). However, the succinyl-group of succinyl-CoA does not point to and locate in the acyl-group binding pocket of HBO1 due to the bulkier and acidic nature. Instead, the acidic group points to the opposite direction of the acyl-group binding pocket and locates next to residues Glu508 and Cys474 that are responsible for the catalytic activity of HBO1 and also part of the lysine substrate binding tunnel of HBO1 (Figure 2H, I). Thus, the presence of succinyl-group of succinyl-CoA would conflict with the binding of lysine residue of the substrate, thus explaining why HBO1 lacks succinylation activity.

HBO1 is required for bulk histone propionylation, butyrylation and crotonylation in cells

To investigate if HBO1 possesses broad histone acyltransferase activity in cells, we first generated HBO1 knockout (HBO1-KO) cell clones in HeLa cells using CRISPR-Cas9 technology (39) (Supplementary Figure S3A, B). We screened for HBO1 null clones on the basis of lack of detectable HBO1 proteins in WB analysis by four different anti-HBO1 antibodies (Supplementary Figure S3C). Multiple HBO1-KO clones were obtained, and these clones were viable in long-term culture but exhibited a reduced cell proliferation rate and modest changes in cell cycle (Supplementary Figure S3D, E). We prepared core histones from control HeLa cells and two representative HBO1-KO clones by acid extraction and analyzed histone acylation status by WB using pan-acyl-lysine specific antibodies. As shown in Figure 3A, we observed that loss of HBO1 led to a marked reduction of histone acetylation in both H3 and H4, consistent with HBO1 being a major enzyme for cellular histone acetylation (26,33). Importantly, we found that loss of HBO1 also led to a marked reduction of propionylation, butyrylation as well as crotonylation in both H3 and H4 (Figure 3A). The observed reduction of global histone acylations was most likely the direct result of loss of HBO1 acyltransferase activity, because loss of HBO1 did not significantly alter the levels of other KATs including p300, GCN5, PCAF and MOF in HeLa cells (Figure 3B). Furthermore, by immunofluorescence (IF) staining assay we found that loss of HBO1 did not affect the histone acyltransferase activity of ectopically expressed CBP and MOF (Supplementary Figure S4A, B). In addition, loss of HBO1 also did not reduce the levels of ACLY and ACSS2, the enzymes critical for production of acyl-CoAs in cells (Figure 3B). Furthermore, loss of HBO1 did not significantly alter the levels of lysine acylations on non-histone proteins (Figure 3C and Supplementary Figure S5A), which also likely excludes the possibility that the reduced histone acylations in HBO1-KO cells is due to a lower availability of the respective acyl-CoAs. Despite above results, we could not entirely exclude the possibility that the observed reduction of histone acylations could be secondary to loss of HBO1, as the HBO1 null cells were derived from single cells that had been cultured extensively before subjected to analysis of histone acylations.

To test whether observed global reduction of various histone acylations is a direct effect of loss of HBO1, we also carried out transient knockout of HBO1 in HeLa cells by infection of stable HBO1-sgRNA expressing HeLa cells with adenoviral Cas9 for 2 days. Subsequent WB analysis revealed that transient HBO1 knockout also resulted in substantial reduction of histone acetylation, propionylation, butyrylation and crotonylation (Supplementary Figure S5B). Similarly, we observed that transient knockdown of HBO1 in HeLa and HCT116 cells by HBO1-specific shRNAs recapitulated the results in HBO1-KO cells, leading to marked reduction of not only histone acetylation, but also propionylation, butyrylation and crotonylation in both H3 and H4 (Figure 3D and E). Again, knockdown of HBO1 had no obvious effect on global acetylation, propionylation, butyrylation and crotonylation of non-histone proteins in HeLa (Figure 3F). We found that Hbo1 protein is also required for bulk histone acetylation, propionylation, butyrylation and crotonylation in mouse embryonic stem (mES) cells, as knockdown of Hbo1 in CGR8 mES cells resulted in marked reduction of these histone modifications (Figure 3G, left panel). However, knockdown of Hbo1 did not affect acylations of non-histone proteins in CGR8 cells (Supplementary Figure S5C). Furthermore, knockdown of Hbo1 in CGR8 ES cells also resulted in a marked reduction of Oct4 and Sox2 proteins (Figure 3G, right panel) and significantly diminished mES stemness activity (Figure 3H), consistent with a role of Hbo1 in maintaining pluripotency and self-renewal of embryonic stem cells (65). Thus, these results demonstrate that HBO1 is required for bulk histone acetylation, propionylation, butyrylation and crotonylation in various cell lines including mES cells

To more precisely define the role of HBO1 in bulk histone acylations, we carried out SILAC-based proteomic

Table 2. Summary of diffraction data and refinement statistics

PDB code	Apo 7D0O	Propionyl-CoA 7D0P	Butyryl-CoA 7D0Q	Crotonoyl-CoA 7D0R	Succinyl-CoA 7D0S
Data collection					
Space group	*C*2	*C*2	*C*2	*C*2	*C*2
Cell dimensions					
a (Å)	127.6	126.7	126.9	127.3	127.1
b (Å)	38.4	39.3	39.6	39.6	39.6
c (Å)	88.1	87.7	87.9	88.1	88.3
α (°)	90.0	90.0	90.0	90.0	90.0
β (°)	122.6	123.0	122.9	123.2	122.9
γ (°)	90.0	90.0	90.0	90.0	90.0
Resolution (Å)	50.0–2.50 (2.59–2.50)[a]	50.0–1.80 (1.86–1.80)	50.0–2.20 (2.28–2.20)	50.0–1.95 (2.02–1.95)	50.0–2.30 (2.38–2.30)
Observed reflections	72,557	216,358	120,505	167,713	92 944
Unique reflections (I / $\sigma(I) > 0$)	11 980 (912)	33 222 (3140)	18 377 (1836)	26 858 (2647)	16 040 (1280)
*R*merge (%)[b]	9.7 (36.5)	5.0 (58.6)	9.1 (56.0)	7.1 (70.3)	10.1 (77.2)
$I/\sigma(I)$	25.9 (2.2)	32.2 (2.0)	28.6 (2.4)	38.5 (2.3)	23.3 (2.7)
Completeness (%)	95.0 (73.8)	98.0 (94.6)	99.3 (99.9)	97.8 (97.5)	94.7 (76.9)
Redundancy	6.1 (4.8)	6.5 (5.4)	6.6 (6.4)	6.2 (4.9)	5.8 (3.6)
Refinement					
Resolution (Å)	50.0–2.50	50.0–1.80	50.0–2.20	50.0–1.95	50.0–2.30
No. reflections					
Working set	8006	31 519	17 452	25 279	15 165
Test set	415	1638	925	1361	772
Rwork/Rfree (%)[c]	24.3/29.5	17.2/21.8	19.0/24.7	18.3/22.8	19.2/25.4
No. atoms					
Protein	2482	2482	2499	2488	2476
Ligand	-	52	53	53	55
Water	36	102	53	91	14
B-factors					
Protein	40.0	58.1	68.1	55.6	76.9
Ligand	-	43.5	73.3	60.5	81.1
Ion	32.9	45.5	55.5	42.4	64.8
Water	29.9	54.0	61.5	52.6	44.9
R.m.s. deviations					
Bond lengths (Å)	0.007	0.008	0.006	0.010	0.007
Bond angles (°)	1.2	1.3	1.1	1.3	1.2
Ramachandran plot (%)					
Favored	93.2	96.9	96.6	96.9	96.2
Allowed	6.8	3.1	3.4	3.1	3.8

[a]Numbers in parentheses represent the highest resolution shell.
[b]$Rmerge = \sum_{hkl}\sum_i|I_i(hkl) - < I(hkl) >|/\sum_{hkl}\sum_i I_i(hkl)$.
[c]$R = \sum_{hkl}||F_o|-|F_c||/\sum_{hkl}|F_o|$.

analysis (66) to quantitatively compare the relative levels of histone acylations in control HeLa and HeLa cells with transient knockdown of HBO1 by shHBO1. We used transient knockdown cells for analysis to minimize the potential secondary effect on histone acylations by long-term loss of HBO1. Core histones were prepared and subjected to mass spectrometry analysis without enrichment of acylated histone peptides with pan acyl-lysine specific antibodies. This analysis identified 21 acetylation, 6 propionylation, 2 butyrylation and none crotonylation sites on histones (Table 3), with the numbers of identified sites most likely reflect the relative abundance of each type of acylation in histones. We normalized the abundance of each modified histone peptides to the various histone peptides with no detected modification (Supplementary Table S3). Notably, knockdown of HBO1 reduced the levels of acetylation, propionylation and butyrylation at nearly all sites to various extent except H3K23ac, and all of the differences are statistically highly significant (Table 3). Consistently with our WB data, H3K14pr is among the most significant reduced modifications in histones upon knockdown of HBO1. Thus, the SILAC experiments unambiguously demonstrated a role of HBO1 in bulk histone acetylation, propionylation as well as butyrylation. We failed to identify crotonylated histone peptides in our SILAC assay because crotonylation is in low abundance and required additional step of peptide enrichment by pan crotonyl-lysine specific antibody for detection by mass spectrometry.

The intrinsic acyltransferase activity of HBO1 mediates bulk histone propionylation, butyrylation and crotonylation in cells

Although the JADE-containing HBO1 complexes preferentially acetylate histone H4 in chromatin, HBO1 is essential for histone H3 lysine 14 acetylation (H3K14ac) but is dispensable for H4 acetylation in mouse embryos (28). A recent study in human cells also concludes that HBO1 is essential for H3K14ac but not the others (31). Although reduced acetylation in histone H4 was observed in their study, this

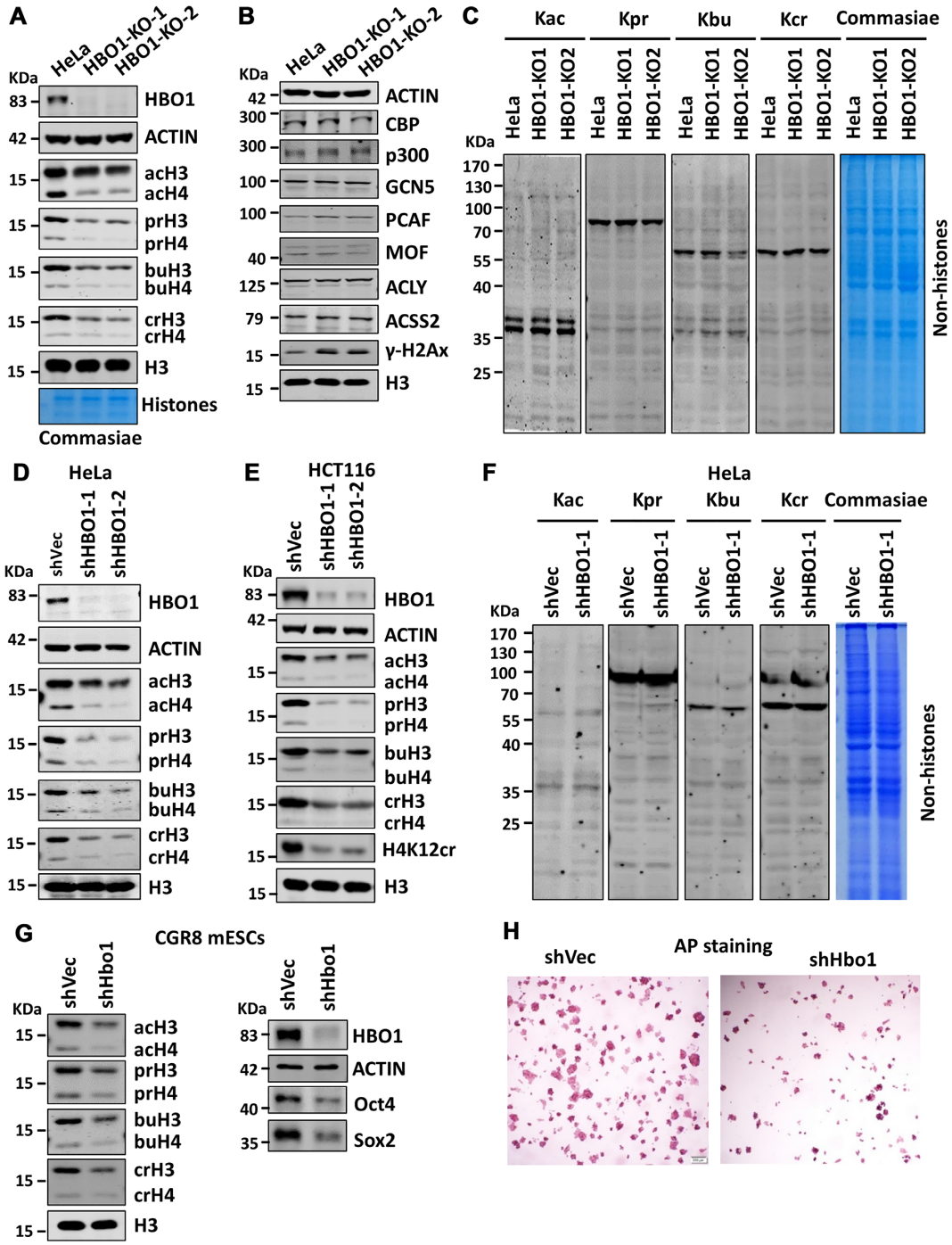

Figure 3. Characterization of HBO1 histone acyltransferase activities in cells. (**A**) WB analysis showing substantial reduction of histone acetylation, propionylation, butyrylation and crotonylation in two HBO1-KO HeLa cell lines. (**B**) WB analysis showing that loss of HBO1 had no significant effect on the levels of CBP, p300, GCN5, PCAF, MOF, ACLY and ACSS2. Note loss of HBO1 resulted in an increase of γ-H2x. (**C**) WB analysis examining the effect of HBO1 knockout on non-histone protein acylations. Whole cell extracts were used for WB analysis. (**D**, **E**) WB analysis showing the effect of transient HBO1 knockdown by lentiviral-based shRNAs on global histone acylations in HeLa cells (D) and HCT116 cells (E). (**F**) WB analysis showing that knockdown of HBO1 by lentiviral-based shRNA had no obvious effect on the levels of global non-histone protein acylations. Whole cell extracts were used for WB analysis. (**G**) WB analysis showing the effect of knockdown of Hbo1 on histone acylations and expression of Oct4 and Sox2 proteins in mouse CGR8 ES cells. (**H**) AP staining assay showing that knockdown of Hbo1 impaired CGR8 ES cell self-renewal capability.

Table 3. Summary of histone acylation changes in HBO1 knockdown HeLa cells determined by SILAC assay

Sites	H	L	Ratio H/L	Normalized ratio H/L
H3K9ac	3.30E+08	5.17E+08	0.64	**0.59**
H3K14ac	1.51E+09	2.10E+09	0.72	**0.67**
H3K23ac	1.31E+09	1.16E+09	1.13	**1.04**
H3K27ac	5.08E+07	7.11E+07	0.71	**0.66**
H2AK5ac	3.01E+06	4.63E+06	0.65	**0.63**
H2BK5ac	1.82E+07	2.58E+07	0.71	**0.72**
H2BK11ac	1.60E+06	2.11E+06	0.76	**0.78**
H2BK12ac	1.60E+06	2.11E+06	0.76	**0.78**
H2BK16ac	6.88E+07	7.95E+07	0.86	**0.89**
H2BK20ac	2.36E+08	2.84E+08	0.83	**0.85**
H2BK34ac	6.52E+05	7.20E+05	0.91	**0.93**
H2BK46ac	1.44E+06	1.59E+06	0.91	**0.93**
H2BK108ac	5.08E+05	9.16E+05	0.55	**0.57**
H2BK120ac	5.68E+05	8.18E+05	0.70	**0.71**
H4K5ac	6.55E+07	1.02E+08	0.64	**0.64**
H4K8ac	9.07E+07	1.31E+08	0.69	**0.70**
H4K12ac	1.46E+08	2.20E+08	0.66	**0.66**
H4K16ac	8.20E+07	1.44E+08	0.57	**0.57**
H4K31ac	2.89E+06	3.95E+06	0.73	**0.73**
H4K77ac	1.71E+06	2.04E+06	0.84	**0.84**
H4K91ac	1.27E+06	1.61E+06	0.79	**0.79**
H3K9pr	2.79E+05	3.57E+05	0.78	**0.72**
H3K14pr	2.70E+05	4.58E+05	0.59	**0.55**
H3K27pr	3.65E+05	5.36E+05	0.68	**0.63**
H2BK34pr	4.01E+05	5.73E+05	0.70	**0.72**
H4K31pr	1.87E+07	2.04E+07	0.92	**0.92**
H4K79pr	8.09E+06	8.42E+06	0.96	**0.96**
H3K9bu	4.11E+05	6.74E+05	0.61	**0.57**
H3K27bu	2.53E+06	2.58E+06	0.98	**0.91**

H: stable heavy isotope labeled HBO1 knockdown cells.
L: stable light isotope labeled control cells.
Ac, acetylation; pr, propionylation; bu, butyrylation.
The SILAC assay was carried out as described in Materials and Methods. Ratio H/L represents the raw ratio of heavy isotope labeled vs lighted isotope labeled histone peptides containing the particular acylated site. Normalized H/L ratio represents the ratio after normalization for the amount of heavy isotope labeled versus light isotope labeled histone proteins. Also shown are statistical significance of SILAC quantified data for heavy isotope labeled and light isotope labeled samples.

was explained as the secondary effect of loss of H3K14ac. As reduction of acetylation, propionylation, butyrylation and crotonylation was observed in both H3 and H4 by WB and in all core histones by SILAC in either permanent HBO1 knockout or transient knockdown cells, we wished to determine if this is intrinsic to HBO1 acyltransferase activity. To this end, we performed 'rescue' experiments in HBO1 knockout cells by re-expressing either wild-type HBO1 or E508Q mutant by lentivirus-based infection, which resulted in ectopic expression of either wild-type HBO1 or E508Q mutant in 100% cells. WB analysis was performed 4 days after viral infection and the representative results showed that re-expression of wild-type HBO1 fully restored all histone acylation defects in HBO1 knockout cells (Figure 4A). However, re-expression of E508Q mutant rescued none of the defects in histone acylations. WB analysis using site-specific antibodies confirmed that re-expression of wild-type HBO1 but not the E508Q mutant rescued acetylation and propionylation on H3K14 and acetylation and butyrylation on H4K12 (Figure 4A). To test the ability for both wild-type HBO1 or E508Q mutant to rescue histone acylations by IF staining assay, we transfected HBO1-KO cells with plasmids encoding either wild-type HBO1 or E508Q mutant. Subsequent IF analysis showed that ectopic expression of wild-type HBO1 but not E508Q mutant drastically elevated the levels of lysine acetylation, propionylation, butyrylation and crotonylation in HBO1-KO HeLa cells (Figure 4B). Together these data demonstrated that the intrinsic enzymatic activity is required for HBO1-dependent bulk histone acylations.

It is noteworthy that, unlike the case in HBO1-KO cells in which ectopic expression of HBO1 alone led to elevated levels of acylations (Figure 4B), ectopic expression of HBO1 alone in control HeLa cells did not elevate the levels of acylations (Supplementary Figure S6A). This discrepancy is likely due to a dependence of HBO1 acyltransferase activity on the formation of scaffold-containing protein complexes (35,64,67) (see next). In control HeLa cells, endogenous scaffold proteins (BRPFs and JADEs) are likely limited and occupied with HBO1 or other members of MYST KATs. Ectopic expressed HBO1 is therefore inactive because no free scaffold protein is available to form the functional HBO1 complex. In HBO1-KO cells, the scaffold proteins become available due to absence of endogenous HBO1, and ectopic expressed HBO1 becomes functionally active because it can now associate with free scaffold proteins to form the scaffold-containing HBO1 complexes.

The scaffold proteins are required for HBO1 acyltransferase activity in cells

As purified HBO1 alone is poorly active in histone acylation assay *in vitro* (Figure 1B) and ectopic expression of HBO1 alone in control HeLa cells failed to elevate histone acylations (Supplementary Figure S6A), we next investigated if HBO1 catalyzes histone acylations in a scaffold protein-dependent manner. Consistent with this idea, IF staining analysis showed that, in the contrary to the situation of expression of HBO1 alone, co-expression of JADE1 and HBO1 resulted in marked elevation of lysine acetylation, propoionylation, butyrylation as well as crotonylation in HeLa cells (Figure 4C, left panel). As a control, expression of JADE1 alone had no effect on lysine acetylation, propoionylation, butyrylation as well as crotonylation (Figure 4C, right panel). Similarly, we found that while expression of BRPF2 alone had no effect on cellular acylations, co-expression of BRPF2 and HBO1 also markedly elevated the levels of lysine acetylation, propoionylation, butyrylation as well as crotonylation in HeLa cells (Supplementary Figure S6B). We observed that, when expressed alone, FLAG-BRPF2 was resided primarily in cytoplasm. Co-expression of FLAG-BRPF2 with Myc-HBO1 resulted in FLAG-BRPF2 nuclear localization, presumably due to the formation of BRPF2–HBO1 complex (Supplementary Figure S6B). Thus, both JADE1 and BRPF2 scaffold proteins are capable of potentiating HBO1 acyltransferase activity in cells.

A caveat for the above IF staining assay is that the observed acyltransferase activity might not directly represent the histone acyltransferase activity of HBO1, as we could not exclude the possibility that the resulting HBO1 complexes also catalyze acylations on non-histone nuclear pro-

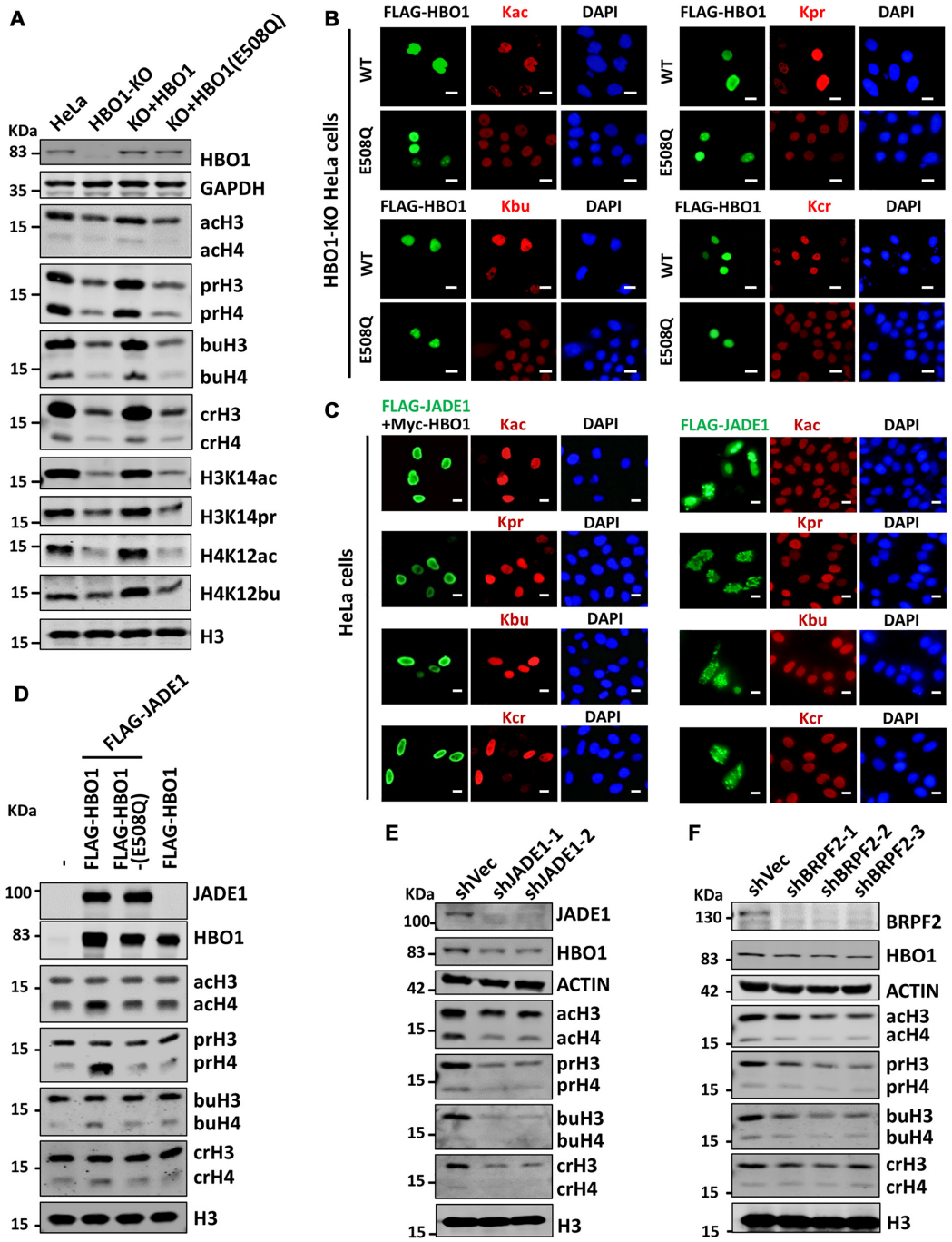

Figure 4. The intrinsic enzymatic activity and scaffold proteins are required for HBO1-mediated histone acylations. (**A**) WB analysis showing that re-expression of wildtype but not E508Q mutant HBO1 rescued histone acylations in HBO1-KO cells. HBO1-KO HeLa cells were infected with lentiviruses encoding wildtype or E508 mutant HBO1 and treated with puromycin to select for lentivirus- infected cells. Core histones were then prepared from cells by acid extraction and subjected to WB analysis using antibodies as indicated. (**B**) IF staining analysis showing that ectopic expression of wildtype but not E508Q mutant HBO1 rescued histone acylations in HBO1-KO cells. HBO1-KO HeLa cells were transfected with plasmids expressing either FLAG-HBO1 or FLAG-HBO1(E508Q) as indicated and 2 days after transfection the cells were processed for double IF staining analysis for FLAG-tagged proteins and each type of the acylations using corresponding pan acyl-lysine antibodies as indicated. Scale bars, 20μm. (**C**) IF staining analysis showing that ectopic expression of JADE1 activated HBO1 acyltransferase activity in HeLa cells. HeLa cells were transfected with plasmids expressing either FLAG-JADE1 alone or together with Myc-HBO1 as indicated and two days after transfection the cells were processed for double IF staining analysis for FLAG-JADE1 and each type of the acylations using corresponding pan acyl-lysine antibodies as indicated. Note that ectopic expression of either HBO1 alone (Supplementary Figure S4A) or JADE1 alone (right panel) did not elevate the levels of acylations above the control untransfected cells. However, co-expression of JADE1 and HBO1 (left panel) markedly elevated the levels of acylations in transfected cells. Scale bars, 20 μm. (**D**) WB analysis co-expression of JADE1 with wildtype but not E508Q mutant HBO1 markedly elevated histone acylations, especially on histone H4, in HEK293T cells. Also note that expression of HBO1 alone had not obvious effect on global histone acylations. (**E**, **F**) WB analysis showing that knockdown of either JADE1 or BRPF2 reduced the levels of histone acylations in HeLa cells. HEK293T cells were infected by lentiviruses encoding either shJADE1 (E) or shBRPF2 (F). Four days after infection core histones were prepared and subjected to WB analysis using antibodies as indicated.

teins. To assess specifically histone acylations, we thus prepared core histones by acid extraction from HEK293T cells that ectopically expressed wild-type HBO1 or E508Q mutant alone or together with JADE1. Subsequent WB analysis showed that co-expression of JADE1 with wild-type HBO1 led to substantial increase of histone H4 acetylation, propionylation, butyrylation and crotonylation (Figure 4D), consistent with our data that the JADE1/HBO1 complex preferentially catalyzes H4 acylations in nucleosome (Figure 1D). However, neither expression of HBO1 alone nor co-expression of E508Q HBO1 mutant plus JADE1 resulted in elevation of histone acylations (Figure 4D), indicating that the observed histone acyltransferase activity for co-expressed JADE1–HBO1 complex is dependent on both HBO1's intrinsic enzymatic activity and the presence of JADE1 scaffold protein. Knockdown of JADE1 led to clear reduction of bulk histone acetylation, propionylation, butyrylation and crotonylation (Figure 4E), suggesting that the JADE1/HBO1 may represent the major HBO1 complex in HeLa cells. Interestingly, knockdown of JADE1 also reduced the level of HBO1 protein (Figure 4E), suggesting that JADE1 is likely required for HBO1 protein stability. In addition, we found that knockdown of BRPF2 also reduced bulk histone acylations, although to a less extent in comparison to JADE1 knockdown (Figure 4F). Thus, both gain and loss of function assays indicate that the JADE and BRPF family scaffold proteins are required for potentiating HBO1 histone acyltransferase activity in cells.

HBO1 and CBP/p300 catalyze acylations on both overlapping and unique sites of histones

CBP and p300 are not only the most versatile histone acyltransferases characterized so far (12), but are also recognized as the major acyltransferase in cells (21). Having demonstrated that HBO1 is required for bulk histone acylations in cells, we wished to characterize its relative contribution and substrate specificity in comparison to CBP/p300. We observed in HeLa cells that knockdown of CBP by specific shRNA reduced the bulk histone acetylation, propionylation, butyrylation and crotonylation to a similar extent as that of HBO1 knockout (Figure 5A). Furthermore, we found that knockdown of CBP in HBO1-KO cells led to further reduction of bulk histone acetylation, propionylation, butyrylation and crotonylation (Figure 5B), indicating that CBP and HBO1 act independently in histone acylations. To compare both CBP/p300 activity with that of HBO1, we treated both control and HBO1-KO cells with A-485, a potent and selective CBP/p300 inhibitor (68). The representative results in Figure 5C show that inhibition of CBP/p300 led to marked global reduction of histone acylations in both control and HBO1-KO cells. Notably, inhibition of CBP/p300 by A-485 did not significantly affect the levels of H3K14ac and H3K14pr in control cells, whereas both modifications were severely reduced in HBO1-KO cells. On the other hand, H3K18ac, which is not reduced by loss of HBO1, is markedly inhibited by A-485. These results therefore suggest that, while both CBP/p300 and HBO1 contribute to bulk histone acylations in cells, they exert on overlapping as well as distinct sites. To investigate this further, we compared in more detail the histone acylation status in CBP knockdown and HBO1 KO cells. As shown in Figure 5D, loss of HBO1 did not affect H3K4cr, H3K9ac/cr, H3K18ac/pr/cr, H4K5ac/bu and H2BK120ac, but led to marked reduction of H3K14ac/pr/cr and H4K12ac/bu/cr, On the other hand, knockdown of CBP led to reduced H3K4cr, H3K9cr, H3K18ac/cr, H4K12ac and H2BK120ac and had little effect on other tested sites. As it was demonstrated before that HBO1 is required for H3K14ac and contributes to H4K12ac, our results reveal that HBO1 is responsible for bulk histone acylations on H3K14 and also contributes to bulk histone acylations on H4K12 site. We noticed increased H3K9ac and H3K9cr in HBO1-KO cells (Figure 5D) and this was not observed in our SILAC analysis with histones from transient HBO1 knockdown cells, suggesting these aberrant modifications are likely due to the secondary effect of HBO1 knockout.

To determine unbiasedly the site specificity of the HBO1complexes, we analyzed by mass spectrometry the acylated sites on core histones catalyzed *in vitro* by purified nBRPF2–HBO1 and JADE1–HBO1 complexes with individual acyl-CoA as in Figure 1. All identified acylation sites were summarized Table 4, and all histone acylation peptides catalyzed by nBRPF2–HBO1 and by JADE1–HBO1 were shown in Supplementary Table S4 and Supplementary Table S5, respectively. Thus, both types of complexes were able to catalyze acetylation on majority of lysine residues in H3 and H4 N-terminal tails. Interestingly, nBRPF2–HBO1 appeared to preferentially acetylate H2A, whereas JADE1–HBO1 complex seems to preferentially acetylate H2B. Similarly, both complexes catalyzed propionylation on multiple sites of histones H3 and H4. For butyrylation, three sites for H3 and two for H4 were identified in the reactions with JADE1–HBO1, whereas only one H3 site was identified in the reactions with nBRPF2–HBO1. For crotonylation, only a single site, H4K12, was identified in the reaction with nBRPF2–HBO1 and none for JADE1–HBO1. As these *in vitro* acylation reactions were carried out with the same concentration of acyl-CoA (100 μM), the results represent by far the most comprehensive characterization of histone acylation site specificity for HBO1 complexes *in vitro* and clearly demonstrate that the HBO1 complexes possess histone acylation activity in an order of acetylation > propionylation > butyrylation > crotonylation activity. These results demonstrate that, similar to CBP/p300 (22), the acyltransferase activity of HBO1 becomes progressively weaker with increased length of acyl chain.

HBO1 is highly enriched at and broadly required for histone acylations on TSSs

We next wished to determine if and how HBO1 contributes histone acylation landscapes in mammalian genome. To this end, we first performed chromatin immunoprecipitation followed by high-throughput DNA sequencing (ChIP-seq) for HBO1 in both control and HBO1-KO HeLa cells. The two replicates of HBO1 in both conditions had Pearson's correlation coefficients > 0.87, indicating the high reproducibility of the HBO1 ChIP-seq data (Supplementary Figure S7). Using MACS2 peak calling algorithm (*64*), a total of 11051 HBO1 peaks were identified in control HeLa cells. To our

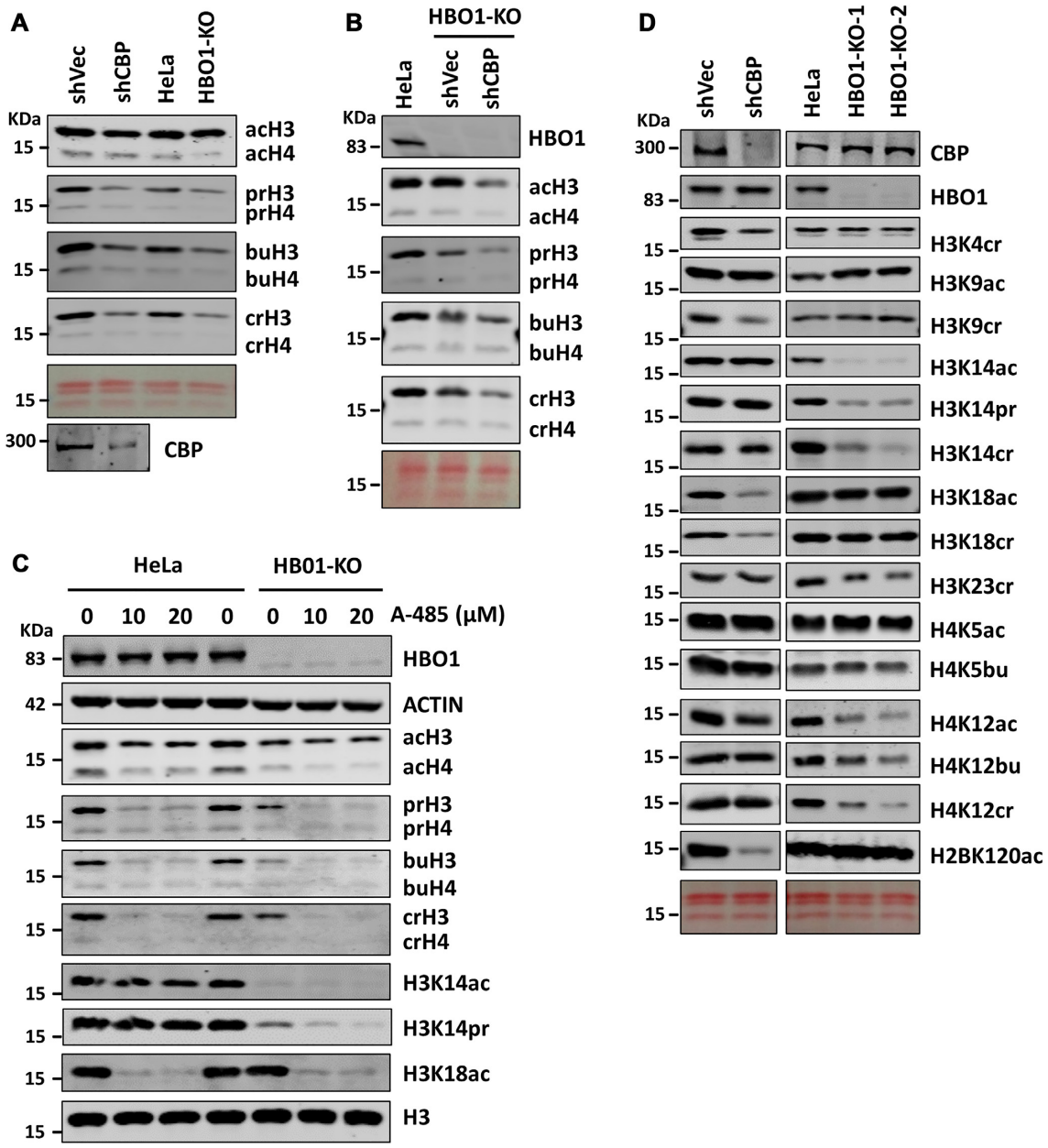

Figure 5. Comparison of HBO1 and CBP/p300 site-specificity on histone acylations. (**A**) WB analysis comparing the levels of histone acylations in CBP knockdown and HBO1 knockout cells. (**B**) WB analysis showing that knocking down CBP in HBO1-KO cells resulted in further reduction of histone acylations. (**C**) WB analysis showing that treatment with CBP/p300 specific inhibitor A-485 resulted in further reduction of histone acylations in HBO1-KO HeLa cells. Cells were treated with A-485 at a concentration of 0, 10 or 20 μM as indicated for 12 h. (**D**) Side-by-side comparison of histone acylation profiles in CBP knockdown and HBO1-KO cells by WB analysis.

delight, nearly all HBO1 peaks observed in control HeLa cells were lost in HBO1-KO cells, thus validating the genuine authenticity of the identified HBO1 peaks. Remarkably, 79.39% of the identified HBO1 peaks can be mapped to TSSs and 85.59% of the peaks were located within 3 kb of TSSs (Figure 6A). To analyze if HBO1 plays a role in histone acylations in TSSs and transcription, we also carried out ChIP-seq analysis for the largest subunit of RNA Pol II, H3K14ac and H3K14cr. Since the H3K14pr antibody was not suitable for ChIP assay in our pilot test, we performed ChIP-seq analysis using pan-Kpr and pan-Kcr antibodies, as these antibodies were suitable for ChIP assay in our tests and likely to represent pan propionylation and pan crotonylation of histones, respectively. When these data were aligned together, we found their peaks show a remarkable co-localization with HBO1 peaks (Figure 6B). The co-localization of HBO1, Pol II, Kpr, Kcr, H3K14ac and H3K14cr signals were illustrated with two representative genes in Figure 6C. Importantly, comparison of ChIP-seq data from control and HBO1-KO HeLa cells revealed that loss of HBO1 led to significant reduction of Kpr and H3K14ac peaks at TSSs (Figure 6C-D) and less significant

Table 4. The list of histone acylation sites identified from *in vitro* acylation reactions with nBPRF2–HBO1 and JADE1–HBO1 complexes and individual acyl-CoAs

Acetyl-CoA			Propipnyl-CoA			Butyrl-CoA			Crotonyl-CoA		
	nBRPF2/ HBO1	JADE1/ HBO1		nBRPF2/ HBO1	JADE1/ HBO1		nBRPF2/ HBO1	JADE1/ HBO1		nBRPF2/ HBO1	JADE1/ HBO1
sites			sites			sites			sites		
H3K9ac		√	H3K4pr	√	√	H3K4bu		√	H4K12cr	√	
H3K14ac	√	√	H3K9pr		√	H3K14bu		√			
H3K18ac	√	√	H3K14pr	√	√	H3K27bu		√			
H3K23ac	√	√	H3K18pr		√	H2BK46bu	√	√			
H3K27ac	√	√	H3K23pr	√	√	H4K8bu		√			
H3K36ac	√	√	H3K27pr	√	√	H4K12bu	√	√			
H3K37ac	√	√	H3K36pr	√	√						
H3K56ac	√	√	H3K37pr		√						
H3K79ac		√	H2BK5pr	√							
H2AK4ac	√		H2BK108pr	√	√						
H2AK5ac	√		H2BK116pr	√	√						
H2AK7ac	√		H4K5pr	√	√						
H2AK9ac	√		H4K8pr	√	√						
H2AK13ac	√		H4K12pr	√	√						
H2AK15ac	√		H4K16pr	√	√						
H2AK95ac	√	√	H4K77pr		√						
H2BK5ac	√										
H2BK11ac	√										
H2BK46ac	√	√									
H2BK108ac		√									
H2BK116ac		√									
H2BK120ac		√									
H4K5ac	√	√									
H4K8ac	√	√									
H4K12ac	√	√									
H4K16ac	√	√									
H4K31ac	√	√									
H4K59ac		√									
H4K77ac	√	√									
H4K79ac		√									

effect on Pol II, Kcr and H3K14cr peaks. One interesting observation in our ChIP-seq profiles is that the low levels of H3K14ac and H3K14cr signals observed in regions outside of the TSSs in control cells were essentially completely lost in the HBO1-KO cells, which was best illustrated in representative H3K14ac and H3K14cr tracks in Figure 6C. To validate our ChIP-seq data, we picked four genes with HBO1 peaks at TSSs and carried out ChIP-qPCR analysis and the results are in general consistent with our ChIP-seq data (Figure 6E), supporting that loss of HBO1 led to a significant reduction of histone acylations at the promoter, but had a moderate effect on Pol II. Taken together, these data reveal a predominant association of HBO1 with TSSs and role of HBO1 in histone acylations at the TSS region.

HBO1 is enriched at subset of DNA replication origins

As HBO1 is implicated in regulation of DNA replication (25,29–31), we wished to also analyze if HBO1 is also enriched at replication origins. We recently showed that histone variant H2A.Z epigenetically regulates the licensing and activation of early replication origins (62). To examine the relationship between HBO1 peaks and DNA replication origins, we first defined 34,511 nascent DNA strand (NS) peaks that overlap with H4K20me2 and ORC1 peaks as DNA replication origins (62) (see Materials and Methods). For all 1,1051 HBO1 peaks, 4,033 peaks were found to directly overlap with DNA replication origins and 4,584 peaks around DNA replication origins (within 5 kb) (Figure 6F). As shown in representative example in Figure 6G (upper panel), signal densities of H4K20me2 and NS were highly enriched at HBO1 binding sites (peak summits). Based on the replication timing profile calculated using time-course BrdU-seq data (Figure 6G, lower panel) (62), we found that these HBO1 replication origins were modestly enriched for the earlier replication domains than average (Figure 6H), suggesting that HBO1 may facilitate the activation of DNA replication initiation through its histone acyltransferase activity.

HBO1 is enriched at TSSs of highly expressed genes

To further investigate the role of HBO1 in transcriptional regulation, we also carried out RNA-seq analysis comparing transcription profiles in control and HBO1-KO cells. Three independent sets of RNA-seq were generated for both control and HBO-1 KO cells and the data were highly reproducible (Supplementary Figure S8). This analysis revealed that loss of HBO1 resulted in 768 downregulated and 675 upregulated genes (Figure 7A). Integrated analysis of ChIP-seq and RNA-seq data revealed that downregulated genes in average had a slightly stronger HBO1 enrichment at the TSS regions than upregulated genes, whereas the unaffected genes had a clear weaker enrichment of HBO1 (Figure 7B-C). To better define the relationship between HBO1 binding at TSSs and gene expression, we subdivided HBO1 peaks into five quantiles according to peak intensity and compared the levels of transcription of their associated genes. We found no significant difference in average levels of transcription among the genes with different HBO1 peak in-

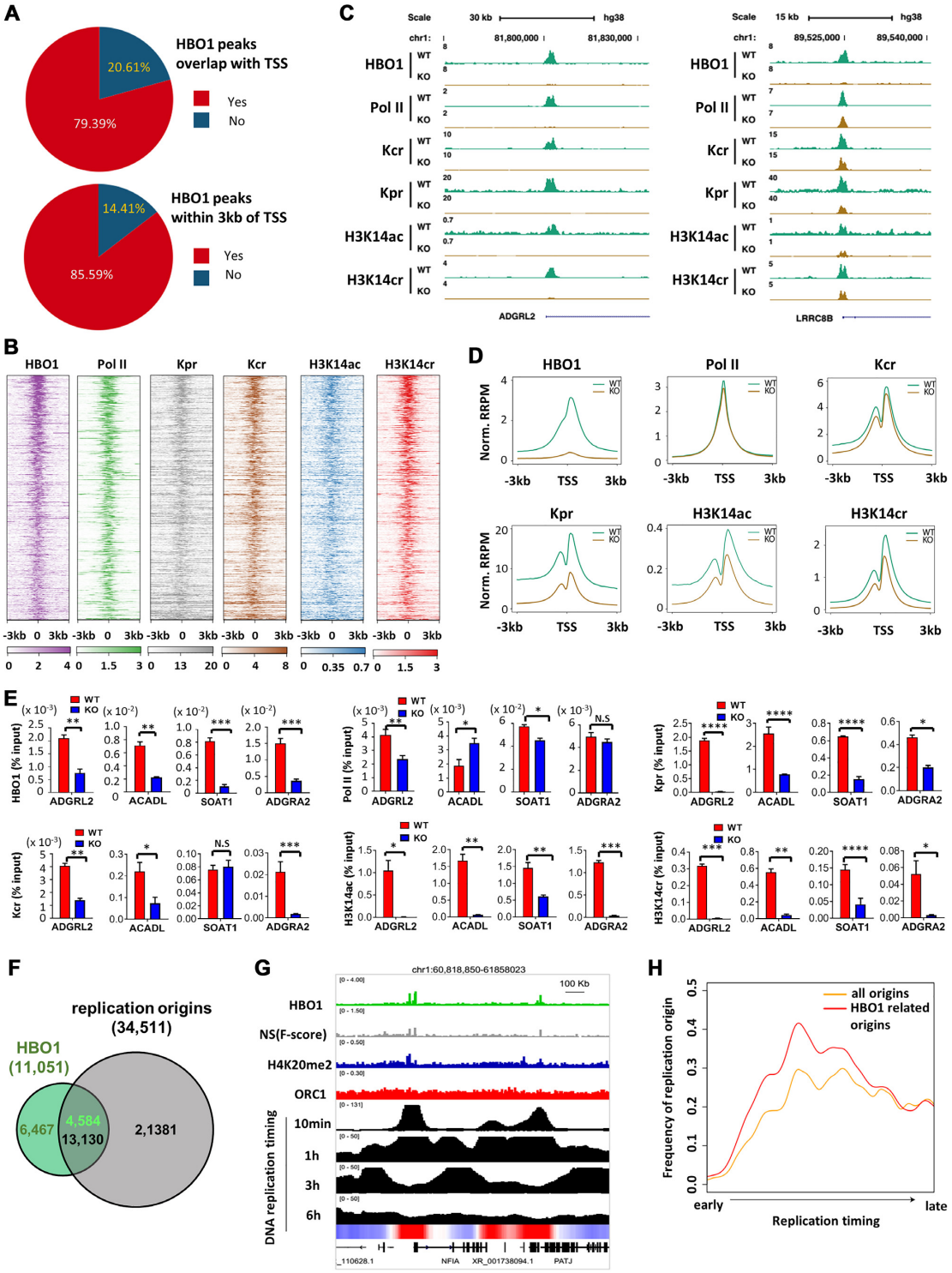

Figure 6. HBO1 contributes to histone acylations in TSSs and partially overlaps with replication origins. (**A**) Venn diagram showing marked enrichment of HBO1 peaks in control HeLa cells identified by ChIP-seq at TSS regions. 79.39% of the total 11051 HBO1 peaks was found to locate at the TSS regions and 85.59% within 3kb of TSS regions. (**B**) Sorted and centered heatmaps generated from ChIP-seq data analysis showing co-occupancy of HBO1, Pol II, Kpr, Kcr, H3K14ac and H3K14cr in HeLa cells. (**C**) Representative tracks showing occupancy of HBO1, Pol II, Kpr, Kcr, H3K14ac and H3K14cr at the TSS regions of genes ADGRL2 and LRRC8B in both control and HBO1-KO cells. Note that the levels of H3K14ac and H3K14cr outside of the TSS regions were essentially completely lost. (**D**) The average plot showing loss of HBO1 led to global reduction of Pol II, Kpr, Kcr, H3K14ac and H3K14cr at the TSS regions. (**E**) Verification of ChIP-seq results by ChIP-qPCR analysis. The results showed that loss of HBO1 resulted in substantial reduction of the levels of Kpr, Kcr, H3K14ac and H3K14cr in the promoter regions of nearly all genes (SOAT1, ADGRA2, ADGRL2 and ACADL) tested. Data are represented as mean of % input ± SD of three biological repeats. (**F**) Venn diagram showing a subset (4584, 41.5%) of HBO1 peaks were around DNA replication origins. (**G**) Representative tracks showing co-occupancy of signals of HBO1, NS, H4K20me2 at early DNA replication regions. (**H**) Histogram shows the replication timing of HBO1-enriched replication origins vs all replication origins.

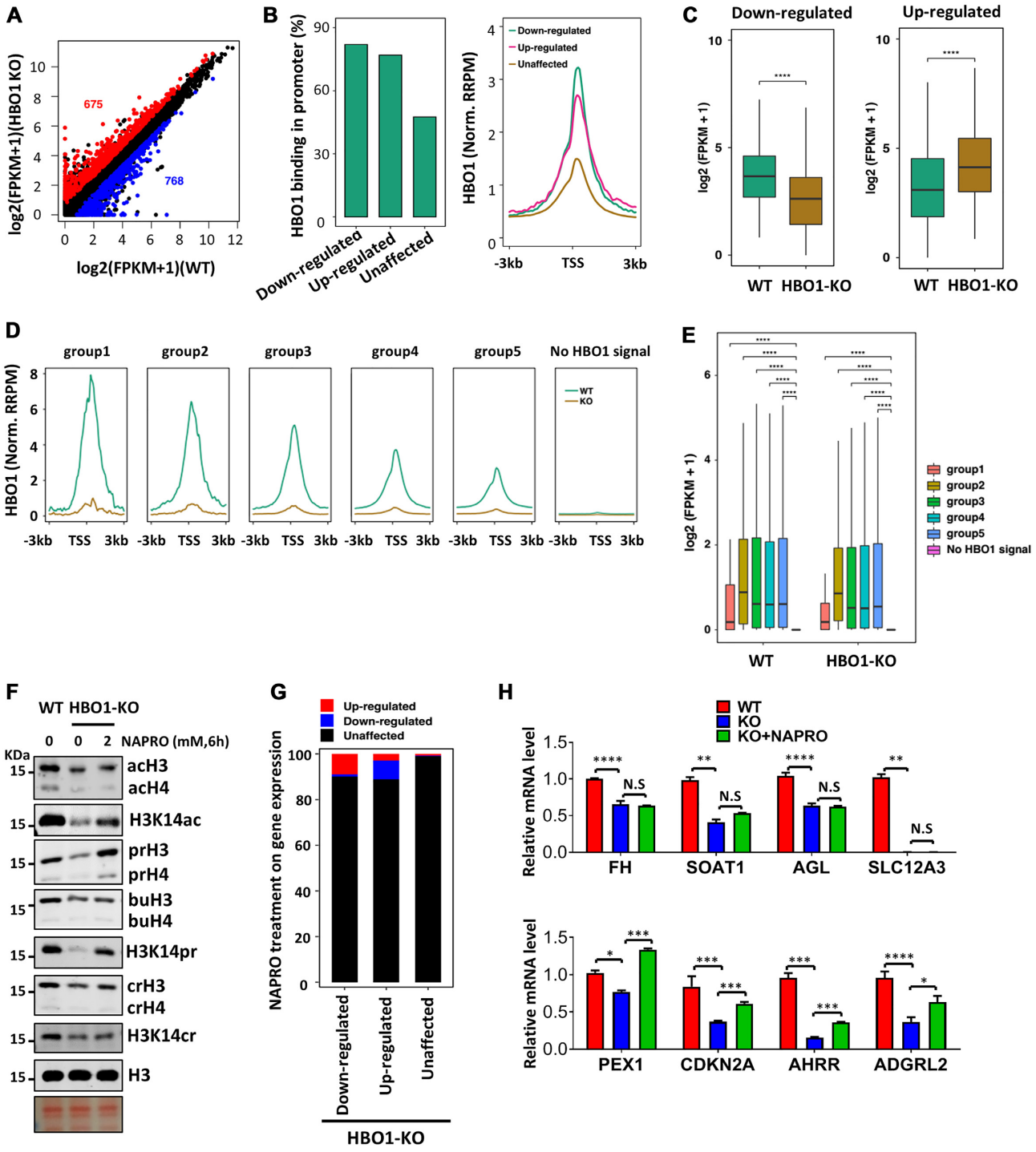

Figure 7. Roles of HBO1 and its association histone acylations in transcription. (**A**) The scatter plot showing 675 up-regulated and 768 down-regulated genes in HBO1-KO cells, with fold change cutoff ≥ 1.5 and *P*-value < 0.05. (**B**) The bar plot and average line plot showing in HeLa cells the relative levels of HBO1 occupancy at the TSSs of genes that were down-regulated, up-regulated, and unaffected in HBO1-KO cells. (**C**) Box plots of expression profiles of genes that were down-regulated (left panel) or up-regulated (right panel) in HBO1-KO cells. (**D**) The average line plots showing six groups of genes that were categorized according to levels of HBO1 peaks intensity at TSSs. (**E**) Box plots showing the relationships between HBO1 peak intensity at TSSs and levels of transcription. (**F**) WB analysis showing that treatment with 2 mM NAPRO for 6 h restored the global histone propionylation in HBO1-KO cells. Note that this treatment did not significantly affect the global levels of histone acetylation, butyrylation and crotonylation. (**G**) RNA-seq analysis showing that NAPRO treatment rescued transcription of a small subset of HBO1-regulated genes. Note that NAPRO treatment had little effect on genes that were not affected by HBO1 knockout. (**H**) RT-qPCR analysis showing rescue of transcription of a subset of down-regulated genes in HBO1-KO cells. Data are represented as relative level of three biological repeats ± SD. **P* < 0.05, ** *P* < 0.01, *** *P* < 0.001, **** *P* < 0.0001, NS, no significant.

tensities at TSS sites (Figure 7D, E). However, the genes without HBO1 peaks at TSS sites were poorly transcribed compared to genes with HBO1 peaks at TSS sites (Figure 7E). Consistent with this observation, we found there is no straight correlation between the levels of HBO1 and the levels of RNA pol II at TSSs (Supplementary Figure S9). However, there is a nice correlation between the levels of HBO1 peaks and the levels of histone acetylation, propionylation and crotonylation at TSSs (Supplementary Figure S9). Thus, our data suggest that HBO1 associates with the TSS sites of transcriptionally active genes and contributes directly to histone acylations at TSSs, yet the recruitment of pol II and the levels of transcription are likely determined by complex parameters other than HBO1 and its associated histone acylations.

Rescue of transcription by restoration of histone propionylation

Our study reveals a potent histone propionylation activity for HBO1. We thus wished to investigate the potential role of histone propionylation in transcriptional regulation by HBO1. To this end, we rescued the global defect of histone propionylation in HBO1-KO cells by addition of sodium propionate (NAPRO), which is expected to be converted into propionyl-coA by acyl-coA synthetase short-chain family member 2 (ACSS2) (20). We found that treatment of HBO1-KO HeLa cells with 2 mM NAPRO was able to restore bulk histone propionylation to a similar extent as in control HeLa cells (Figure 7F and Supplementary Figure S10). Western blotting analysis in Figure 7F also showed that treatment with NAPRO did not significantly affect the levels of histone acetylation, butyrylation and crotonylation in HBO1-KO cells. We then carried out RNA-seq and RT-qPCR analysis of HBO1-regulated genes to examine how restoration of histone propionylation affects gene expression. RNA-seq analysis revealed that NAPRO treatment was able to upregulate 8.85% of down-regulated genes and downregulate 8.44% of up-regulated genes and had little effect on bulk of unaffected genes in HBO1-KO cells (Figure 7G). RT-qPCR analysis of HBO1-KO-down-regulated genes confirmed a partial restoration of transcription for a subset of the downregulated genes in HBO1-KO cells (Figure 7H). Together these data provide evidence that histone propionylation per se may not be able to broadly affect transcription.

DISCUSSION

HBO1 is a versatile and major cellular histone acyltransferase

With the development of start-of-art mass spectrometric technology, an increasing number of short fatty acid modifications on lysine residues, collectively termed as lysine acylations, have been identified on both histones and non-histone proteins (12,69). The continuing quest on enzymes responsible for lysine acylations has led to the findings that CBP and p300 are versatile acyltransferases with activity for propionylation, butyrylation, crotonylation and etc, in addition to their well-recognized acetyltransferase activity (12,13,20–22,70). However, not all acetyltransferases behave as CBP/p300, as GCN5 and PCAF are poorly active in histone butyrylation and crotonylation, despite of their robust propionylation activity, likely due to structural constraints of their CoA binding pockets (23,24). Within the MYST family KATs, we and others have shown that MOF possesses activity for histone propionylation, butyrylation and crotonylation (21,37). In this regard, all members of the MYST family KATs were tested for lysine propionylase activity on histone peptides and cellular proteome in vitro by Han *et al*. and MOF, HBO1 and MOZ were found to have good lysine propionylase activity (37). More recently, MOZ and MORF have been reported to possess robust propionylation activity but are poorly active for butyrylation and crotonylation, and defects in H3 propionylation by MOZ/MORF complexes can lead to neurodevelopmental disorders and cancer (38). In this study, we provide evidence that the BRPF or JADE scaffold containing HBO1 complexes are capable of catalyze histone propionylation, butyrylation, crotonylation, but not succinylation *in vitro* (Figure 1). We show by crystallography that the minimal nBRPF-HBO1 complex is able to accommodate acetyl-, propionyl-, butyl-, crotonyl- and succinyl-CoA with a similar affinity (Figure 2). The structure of succinly-CoA/nBRPF2–HBO1 complex revealed that the presence of succinyl-CoA in the CoA-pocket crashes with binding of substrate lysine residue, thus providing an explanation for the lack of succinylation activity for HBO1.

Our WB analysis of *in vitro* acylation reactions with individual acyl-CoA donor clearly demonstrated that both BRPF2 and JADE-containing HBO1 complexes possess histone propionylation, butyrylation and crotonylation activities (Figure 1). As different and limited numbers of site-specific antibodies were used for WB analysis, however, we cannot tell from this analysis the relative acylation activity and site specificity of HBO1. To overcome this caveat, we also analyzed the resulting core histone products from *in vitro* reactions with an equal concentration of acyl-CoAs by mass spectrometry. This analysis revealed that both nBRPF2–HBO1 and JADE1–HBO1 complexes are able to catalyze acetylation on numerous lysine residues in H3 and H4 N-terminal tails and propionylation on approximately half of the sites (Table 4 and Supplementary Tables S4-S5). However, only 6 butyrylation sites and 1 crotonylation sites were identified (Table 4). Thus, analogous to CBP/p300 (22), our study clearly demonstrates that HBO1's acyltransferase activity becomes progressively weaker when the length of acyl chains of acyl-CoAs increases. The HBO1 acyltransferase activity defined by our *in vitro* assay is in good correlation to the histone acylation profile in cells determined by our SILAC experiments (Table 3). Within a total of 21 acetylated, 6 propionylated, 2 butyrylated and 0 crotonylated histone peptides identified in SILAC from both control and HBO1 knockdown cells (Table 3), 15 acetylated sites and 4 propionylated sites show a more than 20% reduction of modification upon transient knockdown of HBO1, indicating these are the major acylation sites catalyzed by HBO1 complexes in vivo. Furthermore, all these major HBO1 sites identified by SILAC were also identified in *in vitro* histone acylation reactions with nBRPF2–HBO1 and/or JADE1–HBO1 complexes by

mass spectrometry analysis (Table 4 and Supplementary Tables S4 and S5). Thus, both in vivo and in vitro studies demonstrate that HBO1 catalyzes histone acylation with a relatively broad site specificity. Also consistent with previous reports, our SILAC results support that the abundance of histone acylations in cell is in the order of acetylation > propionylation, butyrylation > crotonylation. This histone acylation profile is in part likely explained by the difference in concentrations of acyl-CoAs in cell, with acetyl-CoA > propionyl-CoA> butyryl-CoA> crotonyl-CoA in general (20). Because HBO1 and CBP/p300, which likely comprised of the bulk cellular acyltransferase activity, all show progressively reduced acyltransferase activity toward acyl-CoAs with longer acyl chains, we suggest that this inherent feature of major acyltransferases also contributes to vast difference in abundance of different types of histone acylations in cells.

Our study also suggest that HBO1 is a major histone acyltransferase in cells. Previous studies have established HBO1 as a major histone acetyltransferase in cells (33,71). We show that HBO1 knockout in HeLa cells resulted in substantial reduction of not only histone acetylation, but also histone propionylation, butyrylation and crotonylation. Consistent with previous studies (28,31), we found that HBO1 is required for bulk H3K14ac in cells. Notably, we found that HBO1 is also required for both H3K14pr and H3K14cr, suggesting that HBO1 is responsible for bulk H3K14 acylations in chromatin. In addition, we show that transient knockdown of HBO1 in various cells also resulted in substantial reduction of histone acetylation, propionylation, butyrylation and crotonylation, suggesting the observed global reduction of histone acylations in HBO1-KO cells is unlikely a secondary effect. Nevertheless, some changes of histone acylations in HBO1-KO cells could be secondary. For example, increased H3K9ac and H3K9cr were observed in HBO1-KO cells (Figure 5D) but not in HBO1 KD cells (Table 3), suggesting the increased H3K9ac and H3K9cr could be secondary to HBO1 KO. Furthermore, we show that re-expression of wild-type but not E508Q enzymatic dead mutant rescued histone acylation defect in HBO1-KO cells, indicating the impaired global histone acylations in HBO1-KO cells could be attributed to loss of HBO1. It is noteworthy that knockout or knockdown of HBO1 appears to affect specifically histone acylations, as HBO1 knockout or knockdown had no obvious effect on non-histone protein acylation. This differs from CBP/p300 (21), as they are major acyltransferases for both histone and non-histone proteins.

Although both CBP/p300 and HBO1 are major histone acyltransferases in cells, our study revealed that they catalyze distinct as well as overlapping sites on histones. Our side-by-side analysis of CBP and HBO1 revealed that HBO1 uniquely catalyzes H3K14 acylations, whereas H3K18ac and H3K18cr is unique to CBP. Other sites such as H4K12 are likely catalyzed by both CBP and HBO1. On the global level, it is more evident that inhibition of CBP/p300 activity by A485 inhibitor led to further reduction of global H3 and H4 acylations in HBO1-KO cells. Taken together, these results indicate that HBO1 and CBP/p300 determine bulk histone acylations by catalyzing distinct as well as overlapping sites on histones.

HBO1 is predominantly enriched at TSSs of actively transcribed genes

Previous studies have reported the enrichment of HBO1 or its associated complexes in coding regions of genes and 5' regions of promoters, respectively (26,33). Our ChIP-seq analysis identified 11,051 HBO1 peaks in control HeLa cells and essentially background signals in HBO-KO cells, thus validating the authenticity of the identified HBO1 peaks. Majority of the HBO1 peaks are localized at (79.39%) and/or near (85.59%) the TSS regions of transcribed genes, and exhibit substantial overlap with peaks of pol II, H3K14ac and H3K14cr, as well as with peaks for pan-propionylation and pan-crotonylation antibodies (Figure 6A-B). As our data suggest that HBO1 is highly specific for histone acylations, the detected propionylation and crotonylation peaks at TSSs are most likely to reflect propionylated and crotonylated histone peaks, respectively. Our results demonstrate that HBO1 contributes to histone acylations at TSS regions, as HBO1 knockout resulted in clear reduction of the levels of the acetylation, propionylation and crotonylation at TSS regions. Notably, HBO1 also likely contributes to basal histone acylations throughout the genome, because HBO1 knockout essentially wiped out the genome-wide basal H3K14ac and H3K14cr signals (Figure 6C-D). Thus, our ChIP-seq analysis provides compelling evidence that HBO1 is highly enriched at and contributes to histone acylations at TSS regions. The specific TSS enrichment is most likely mediated by ING4/5 subunits of the HBO1 complexes, as these proteins bind H3K4me3-containing histones with high affinity (33,34).

While our data clearly demonstrate that HBO1 is a predominant enriched and contributes to histone acylations at TSSs, how HBO1 regulates transcription is not clear. Previous studies showed that knockdown or knockout of HBO1 resulted in a similar number of down-regulated and up-regulated genes. Similarly, we observed that knockout of HBO1 resulted in a similar number of down-regulated and up-regulated genes (Figure 7A). Through integrated ChIP-seq and RNA-seq analysis, we observed that HBO1 is highly enriched at TSSs of actively transcribed genes, with little association with TSSs of inactive genes (Figure 7D-E), suggesting a role for HBO1 and its associated histone acylations in potentiating transcription. However, the HBO1 levels at TSSs show no obvious correlation with levels of Pol II and transcription (Figure 7E and Supplementary Figure S9). Furthermore, because both down-regulated and up-regulated genes in HBO1-KO cells were associated with reduced levels of histone acylations at TSSs, HBO1 and its catalyzed histone acylations appear to have roles in both transcriptional activation and repression. Thus, how HBO1 and its associated TSS histone acylations regulate transcription remains unclear and warrants for further study, despite of evidence for a positive correlation between promoter acetylation and levels of transcription (72).

As HBO1 possesses robust histone propionylation activity, we also assess how histone propionylation contributes to transcriptional regulation by HBO1. We found that treatment of HBO1-KO cells with 2 mM NAPRO was able to restore global histone propionylation to a similar level in control cells and had a minimal effect on other types

of histone acylations including acetylation and crotonylation (Figure 7F). Transcriptional analysis revealed that 2 mM NAPRO treatment was able to partially rescue the transcription of a small subset of HBO1-regulated genes (Figure 7G, H). This observation suggests that alteration of histone propionylation per se may not have a broad impact on transcription, although histone propionylation was shown to correlate positively with transcription (73). A caveat for NAPRO treatment is that it is unlikely to fully restore the impaired promoter propionylation due to loss of HBO1, which may partially explain the poor rescue in transcription by NAPRO treatment. Together with the previous studies showing a positive role of histone crotonylation in transcription (15,20,46), a challenge in future would be how to delineate the exact function for each type of acylation and how they act coordinately to regulate transcription.

HBO1 also associates with a subset of replication origins

The identification of genome-wide HBO1 peaks, together with our recent identification of DNA replication origins (62), allowed us to also assess the relationship between HBO1 peaks and replication origins. HBO1 is initially identified as ORC interacting protein (25). There is dispute as to the role of HBO1 in DNA replication, ranging from an essential factor to complete dispensable (29,31,74). We find that approximately 36.5% of HBO1 peaks (4033 out of 11051 HBO1 peaks) are completely overlapped with replication origins, and 41.5% HBO1 peaks (4584 out of 11051 peaks) within 5 kb regions of replication origins. With the facts that HBO1 is present at a subset of replication origins and that HBO1-KO cells are viable, our data support a regulatory role for HBO1 in DNA replication.

DATA AVAILABILITY

All data needed to evaluate the conclusions in the paper are present in the paper and/or the Supplementary Materials. The crystal structures of the HBO1-BRPF2 in apo form, in complexes with propionyl-CoA, butyryl-CoA, crotonoyl-CoA and succinyl-CoA can be accessed in the Protein Data Bank under accession codes 7D0O, 7D0P, 7D0Q, 7D0R and 7D0S, respectively. The raw RNA-seq and ChIP-seq data are publicly accessible at http://bigd.big.ac.cn/gsa-human under accession number HRA000828. Additional data related to this paper may be requested from the corresponding authors.

SUPPLEMENTARY DATA

Supplementary Data are available at NAR Online.

ACKNOWLEDGEMENTS

We thank members of Wong's laboratory for valuable discussion. We also thank the Instruments Sharing Platform of School of Life Sciences, East China Normal University for technical support.

FUNDING

Ministry of Science and Technology of China [2017YFA0504201 to J.W.]; National Natural Science Foundation of China [31961133009 to J.W., 31800622 to J.D., 31801060 to W.W.]; the Shanghai Science and Technology Committee [20JC1411500 to J.W.]; Chinese Academy of Sciences [the Strategic Priority Research Program XDB37030305 to J.D.]. Funding for open access charge: National Natural Science Foundation of China.
Conflict of interest statement. None declared.

REFERENCES

1. Allis,C.D. and Jenuwein,T. (2016) The molecular hallmarks of epigenetic control. *Nat. Rev. Genet.*, **17**, 487–500.
2. Jenuwein,T. and Allis,C.D. (2001) Translating the histone code. *Science*, **293**, 1074–1080.
3. Suganuma,T. and Workman,J.L. (2011) Signals and combinatorial functions of histone modifications. *Annu. Rev. Biochem.*, **80**, 473–499.
4. Vidanes,G.M., Bonilla,C.Y. and Toczyski,D.P. (2005) Complicated tails: histone modifications and the DNA damage response. *Cell*, **121**, 973–976.
5. Roth,S.Y., Denu,J.M. and Allis,C.D. (2001) Histone acetyltransferases. *Annu. Rev. Biochem.*, **70**, 81–120.
6. Shahbazian,M.D. and Grunstein,M. (2007) Functions of site-specific histone acetylation and deacetylation. *Annu. Rev. Biochem.*, **76**, 75–100.
7. Wang,S., Yan-Neale,Y., Zeremski,M. and Cohen,D. (2004) Transcription regulation by histone deacetylases. *Novartis Found. Symp.*, **259**, 238–245.
8. Yang,X.J. (2004) The diverse superfamily of lysine acetyltransferases and their roles in leukemia and other diseases. *Nucleic Acids Res.*, **32**, 959–976.
9. Marmorstein,R. and Trievel,R.C. (2009) Histone modifying enzymes: structures, mechanisms, and specificities. *Biochim. Biophys. Acta*, **1789**, 58–68.
10. Li,B., Carey,M. and Workman,J.L. (2007) The role of chromatin during transcription. *Cell*, **128**, 707–719.
11. Jacobson,R.H., Ladurner,A.G., King,D.S. and Tjian,R. (2000) Structure and function of a human TAFII250 double bromodomain module. *Science*, **288**, 1422–1425.
12. Sabari,B.R., Zhang,D., Allis,C.D. and Zhao,Y. (2017) Metabolic regulation of gene expression through histone acylations. *Nat. Rev. Mol. Cell Biol.*, **18**, 90–101.
13. Chen,Y., Sprung,R., Tang,Y., Ball,H., Sangras,B., Kim,S.C., Falck,J.R., Peng,J., Gu,W. and Zhao,Y. (2007) Lysine propionylation and butyrylation are novel post-translational modifications in histones. *Mol. Cell. Proteomics*, **6**, 812–819.
14. Peng,C., Lu,Z., Xie,Z., Cheng,Z., Chen,Y., Tan,M., Luo,H., Zhang,Y., He,W., Yang,K. *et al.* (2011) The first identification of lysine malonylation substrates and its regulatory enzyme. *Mol. Cell. Proteomics*, **10**, M111.012658.
15. Tan,M., Luo,H., Lee,S., Jin,F., Yang,J.S., Montellier,E., Buchou,T., Cheng,Z., Rousseaux,S., Rajagopal,N. *et al.* (2011) Identification of 67 histone marks and histone lysine crotonylation as a new type of histone modification. *Cell*, **146**, 1016–1028.
16. Zhang,Z., Tan,M., Xie,Z., Dai,L., Chen,Y. and Zhao,Y. (2011) Identification of lysine succinylation as a new post-translational modification. *Nat. Chem. Biol.*, **7**, 58–63.
17. Dai,L., Peng,C., Montellier,E., Lu,Z., Chen,Y., Ishii,H., Debernardi,A., Buchou,T., Rousseaux,S., Jin,F. *et al.* (2014) Lysine 2-hydroxyisobutyrylation is a widely distributed active histone mark. *Nat. Chem. Biol.*, **10**, 365–370.
18. Zhao,S., Zhang,X. and Li,H. (2018) Beyond histone acetylation-writing and erasing histone acylations. *Curr. Opin. Struct. Biol.*, **53**, 169–177.
19. Suganuma,T. and Workman,J.L. (2018) Chromatin and metabolism. *Annu. Rev. Biochem.*, **87**, 27–49.
20. Sabari,B.R., Tang,Z., Huang,H., Yong-Gonzalez,V., Molina,H., Kong,H.E., Dai,L., Shimada,M., Cross,J.R., Zhao,Y. *et al.* (2015)

Intracellular crotonyl-CoA stimulates transcription through p300-catalyzed histone crotonylation. *Mol. Cell*, **58**, 203–215.
21. Liu,X., Wei,W., Liu,Y., Yang,X., Wu,J., Zhang,Y., Zhang,Q., Shi,T., Du,J.X., Zhao,Y. *et al.* (2017) MOF as an evolutionarily conserved histone crotonyltransferase and transcriptional activation by histone acetyltransferase-deficient and crotonyltransferase-competent CBP/p300. *Cell Discov*, **3**, 17016.
22. Kaczmarska,Z., Ortega,E., Goudarzi,A., Huang,H., Kim,S., Marquez,J.A., Zhao,Y., Khochbin,S. and Panne,D. (2017) Structure of p300 in complex with acyl-CoA variants. *Nat. Chem. Biol.*, **13**, 21–29.
23. Leemhuis,H., Packman,L.C., Nightingale,K.P. and Hollfelder,F. (2008) The human histone acetyltransferase P/CAF is a promiscuous histone propionyltransferase. *ChemBioChem*, **9**, 499–503.
24. Ringel,A.E. and Wolberger,C. (2016) Structural basis for acyl-group discrimination by human Gcn5L2. *Acta Crystallogr. D Struct. Biol.*, **72**, 841–848.
25. Iizuka,M. and Stillman,B. (1999) Histone acetyltransferase HBO1 interacts with the ORC1 subunit of the human initiator protein. *J. Biol. Chem.*, **274**, 23027–23034.
26. Avvakumov,N., Lalonde,M.E., Saksouk,N., Paquet,E., Glass,K.C., Landry,A.J., Doyon,Y., Cayrou,C., Robitaille,G.A., Richard,D.E. *et al.* (2012) Conserved molecular interactions within the HBO1 acetyltransferase complexes regulate cell proliferation. *Mol. Cell. Biol.*, **32**, 689–703.
27. Lan,R. and Wang,Q. (2020) Deciphering structure, function and mechanism of lysine acetyltransferase HBO1 in protein acetylation, transcription regulation, DNA replication and its oncogenic properties in cancer. *Cell. Mol. Life Sci.*, **77**, 637–649.
28. Kueh,A.J., Dixon,M.P., Voss,A.K. and Thomas,T. (2011) HBO1 is required for H3K14 acetylation and normal transcriptional activity during embryonic development. *Mol. Cell. Biol.*, **31**, 845–860.
29. Iizuka,M., Matsui,T., Takisawa,H. and Smith,M.M. (2006) Regulation of replication licensing by acetyltransferase Hbo1. *Mol. Cell. Biol.*, **26**, 1098–1108.
30. Miotto,B. and Struhl,K. (2008) HBO1 histone acetylase is a coactivator of the replication licensing factor Cdt1. *Gene Dev*, **22**, 2633–2638.
31. Kueh,A.J., Eccles,S., Tang,L., Garnham,A.L., May,R.E., Herold,M.J., Smyth,G.K., Voss,A.K. and Thomas,T. (2020) HBO1 (KAT7) does not have an essential role in cell proliferation, DNA replication, or histone 4 acetylation in human cells. *Mol. Cell. Biol.*, **40**, e00506-19.
32. Doyon,Y., Cayrou,C., Ullah,M., Landry,A.J., Cote,V., Selleck,W., Lane,W.S., Tan,S., Yang,X.J. and Cote,J. (2006) ING tumor suppressor proteins are critical regulators of chromatin acetylation required for genome expression and perpetuation. *Mol. Cell*, **21**, 51–64.
33. Saksouk,N., Avvakumov,N., Champagne,K.S., Hung,T., Doyon,Y., Cayrou,C., Paquet,E., Ullah,M., Landry,A.J., Cote,V. *et al.* (2009) HBO1 HAT complexes target chromatin throughout gene coding regions via multiple PHD finger interactions with histone H3 tail. *Mol. Cell*, **33**, 257–265.
34. Saksouk,N., Avvakumov,N., Champagne,K.S., Hung,T., Doyon,Y., Cayrou,C., Paquet,E., Ullah,M., Landry,A.J., Cote,V. *et al.* (2009) HBO1 HAT complexes target chromatin throughout gene coding regions via multiple PHD finger interactions with histone H3 tail. *Mol. Cell*, **33**, 257–265.
35. Lalonde,M.E., Avvakumov,N., Glass,K.C., Joncas,F.H., Saksouk,N., Holliday,M., Paquet,E., Yan,K., Tong,Q., Klein,B.J. *et al.* (2013) Exchange of associated factors directs a switch in HBO1 acetyltransferase histone tail specificity. *Genes Dev.*, **27**, 2009–2024.
36. Tao,Y., Zhong,C., Zhu,J., Xu,S. and Ding,J. (2017) Structural and mechanistic insights into regulation of HBO1 histone acetyltransferase activity by BRPF2. *Nucleic Acids Res.*, **45**, 5707–5719.
37. Han,Z., Wu,H., Kim,S., Yang,X., Li,Q., Huang,H., Cai,H., Bartlett,M.G., Dong,A., Zeng,H. *et al.* (2018) Revealing the protein propionylation activity of the histone acetyltransferase MOF (males absent on the first). *J. Biol. Chem.*, **293**, 3410–3420.
38. Yan,K., Rousseau,J., Machol,K., Cross,L.A., Agre,K.E., Gibson,C.F., Goverde,A., Engleman,K.L., Verdin,H., De Baere,E. *et al.* (2020) Deficient histone H3 propionylation by BRPF1-KAT6 complexes in neurodevelopmental disorders and cancer. *Sci. Adv.*, **6**, eaax0021.
39. Ran,F.A., Hsu,P.D., Wright,J., Agarwala,V., Scott,D.A. and Zhang,F. (2013) Genome engineering using the CRISPR-Cas9 system. *Nat. Protoc.*, **8**, 2281–2308.
40. Otwinowski,Z. and Minor,W. (1997) Processing of X-ray diffraction data collected in oscillation mode. *Methods Enzymol.*, **276**, 307–326.
41. Emsley,P. and Cowtan,K. (2004) COOT: model-building tools for molecular graphics. *Acta Crystallogr. D Biol. Crystallogr.*, **60**, 2126–2132.
42. Murshudov,G.N., Vagin,A.A. and Dodson,E.J. (1997) Refinement of macromolecular structures by the maximum-likelihood method. *Acta Crystallogr. D Biol. Crystallogr.*, **53**, 240–255.
43. Adams,P.D., Afonine,P.V., Bunkoczi,G., Chen,V.B., Davis,I.W., Echols,N., Headd,J.J., Hung,L.W., Kapral,G.J., Grosse-Kunstleve,R.W. *et al.* (2010) PHENIX: a comprehensive Python-based system for macromolecular structure solution. *Acta Crystallogr. D Biol. Crystallogr.*, **66**, 213–221.
44. Winn,M.D., Ballard,C.C., Cowtan,K.D., Dodson,E.J., Emsley,P., Evans,P.R., Keegan,R.M., Krissinel,E.B., Leslie,A.G., McCoy,A. *et al.* (2011) Overview of the CCP4 suite and current developments. *Acta Crystallogr. D Biol. Crystallogr.*, **67**, 235–242.
45. Schrödinger,L.L.C. (2015) The PyMOL Molecular Graphics System, Version 2.0 *Schrödinger, LLC*.
46. Wei,W., Liu,X., Chen,J., Gao,S., Lu,L., Zhang,H., Ding,G., Wang,Z., Chen,Z., Shi,T. *et al.* (2017) Class I histone deacetylases are major histone decrotonylases: evidence for critical and broad function of histone crotonylation in transcription. *Cell Res.*, **27**, 898–915.
47. Shechter,D., Dormann,H.L., Allis,C.D. and Hake,S.B. (2007) Extraction, purification and analysis of histones. *Nat. Protoc.*, **2**, 1445–1457.
48. Nie,L., Shuai,L., Zhu,M., Liu,P., Xie,Z.F., Jiang,S., Jiang,H.W., Li,J., Zhao,Y., Li,J.Y. *et al.* (2017) The landscape of histone modifications in a High-Fat Diet-Induced Obese (DIO) mouse model. *Mol. Cell. Proteomics*, **16**, 1324–1334.
49. Yu,M., Yang,W., Ni,T., Tang,Z., Nakadai,T., Zhu,J. and Roeder,R.G. (2015) RNA polymerase II-associated factor 1 regulates the release and phosphorylation of paused RNA polymerase II. *Science*, **350**, 1383–1386.
50. Langmead,B. and Salzberg,S.L. (2012) Fast gapped-read alignment with Bowtie 2. *Nat. Methods*, **9**, 357–359.
51. Orlando,D.A., Chen,M.W., Brown,V.E., Solanki,S., Choi,Y.J., Olson,E.R., Fritz,C.C., Bradner,J.E. and Guenther,M.G. (2014) Quantitative ChIP-Seq normalization reveals global modulation of the epigenome. *Cell Rep.*, **9**, 1163–1170.
52. Zhang,Y., Liu,T., Meyer,C.A., Eeckhoute,J., Johnson,D.S., Bernstein,B.E., Nusbaum,C., Myers,R.M., Brown,M., Li,W. *et al.* (2008) Model-based analysis of ChIP-Seq (MACS). *Genome Biol.*, **9**, R137.
53. Thorvaldsdottir,H., Robinson,J.T. and Mesirov,J.P. (2013) Integrative Genomics Viewer (IGV): high-performance genomics data visualization and exploration. *Brief. Bioinform.*, **14**, 178–192.
54. Kim,D., Paggi,J.M., Park,C., Bennett,C. and Salzberg,S.L. (2019) Graph-based genome alignment and genotyping with HISAT2 and HISAT-genotype. *Nat. Biotechnol.*, **37**, 907–915.
55. Anders,S., Pyl,P.T. and Huber,W. (2015) HTSeq–a Python framework to work with high-throughput sequencing data. *Bioinformatics*, **31**, 166–169.
56. Robinson,M.D., McCarthy,D.J. and Smyth,G.K. (2010) edgeR: a Bioconductor package for differential expression analysis of digital gene expression data. *Bioinformatics*, **26**, 139–140.
57. Wang,Y., Song,F., Zhu,J., Zhang,S., Yang,Y., Chen,T., Tang,B., Dong,L., Ding,N., Zhang,Q. *et al.* (2017) GSA: Genome Sequence Archive. *Genomics Proteomics Bioinformatics*, **15**, 14–18.
58. National Genomics Data Center, M. and Partners. (2020) Database resources of the national genomics data center in 2020. *Nucleic Acids Res.*, **48**, D24–D33.
59. Li,H., Handsaker,B., Wysoker,A., Fennell,T., Ruan,J., Homer,N., Marth,G., Abecasis,G., Durbin,R. and Genome Project Data Processing, S. (2009) The sequence Alignment/Map format and SAMtools. *Bioinformatics*, **25**, 2078–2079.
60. Rozowsky,J., Euskirchen,G., Auerbach,R.K., Zhang,Z.D., Gibson,T., Bjornson,R., Carriero,N., Snyder,M. and Gerstein,M.B. (2009)

PeakSeq enables systematic scoring of ChIP-seq experiments relative to controls. *Nat. Biotechnol.*, **27**, 66–75.
61. Quinlan,A.R. (2014) BEDTools: The Swiss-Army tool for genome feature analysis. *Curr Protoc Bioinformatics*, **47**, 11.12.1–11.12.34.
62. Long,H., Zhang,L., Lv,M., Wen,Z., Zhang,W., Chen,X., Zhang,P., Li,T., Chang,L., Jin,C. *et al.* (2020) H2A.Z facilitates licensing and activation of early replication origins. *Nature*, **577**, 576–581.
63. Ramirez,F., Dundar,F., Diehl,S., Gruning,B.A. and Manke,T. (2014) deepTools: a flexible platform for exploring deep-sequencing data. *Nucleic Acids Res.*, **42**, W187–W191.
64. Foy,R.L., Song,I.Y., Chitalia,V.C., Cohen,H.T., Saksouk,N., Cayrou,C., Vaziri,C., Cote,J. and Panchenko,M.V. (2008) Role of Jade-1 in the histone acetyltransferase (HAT) HBO1 complex. *J. Biol. Chem.*, **283**, 28817–28826.
65. Kim,M.S., Cho,H.I., Park,S.H., Kim,J.H., Chai,Y.G. and Jang,Y.K. (2015) The histone acetyltransferase Myst2 regulates nanog expression, and is involved in maintaining pluripotency and self-renewal of embryonic stem cells. *FEBS Lett.*, **589**, 941–950.
66. Harsha,H.C., Molina,H. and Pandey,A. (2008) Quantitative proteomics using stable isotope labeling with amino acids in cell culture. *Nat. Protoc.*, **3**, 505–516.
67. Mishima,Y., Miyagi,S., Saraya,A., Negishi,M., Endoh,M., Endo,T.A., Toyoda,T., Shinga,J., Katsumoto,T., Chiba,T. *et al.* (2011) The Hbo1-Brd1/Brpf2 complex is responsible for global acetylation of H3K14 and required for fetal liver erythropoiesis. *Blood*, **118**, 2443–2453.
68. Lasko,L.M., Jakob,C.G., Edalji,R.P., Qiu,W., Montgomery,D., Digiammarino,E.L., Hansen,T.M., Risi,R.M., Frey,R., Manaves,V. *et al.* (2017) Discovery of a selective catalytic p300/CBP inhibitor that targets lineage-specific tumours. *Nature*, **550**, 128–132.
69. Huang,H., Lin,S., Garcia,B.A. and Zhao,Y. (2015) Quantitative proteomic analysis of histone modifications. *Chem. Rev.*, **115**, 2376–2418.
70. Huang,H., Tang,S., Ji,M., Tang,Z., Shimada,M., Liu,X., Qi,S., Locasale,J.W., Roeder,R.G., Zhao,Y. *et al.* (2018) p300-Mediated lysine 2-hydroxyisobutyrylation regulates glycolysis. *Mol. Cell*, **70**, 663–678.
71. Sapountzi,V. and Cote,J. (2011) MYST-family histone acetyltransferases: beyond chromatin. *Cell. Mol. Life Sci.*, **68**, 1147–1156.
72. Nicolas,D., Zoller,B., Suter,D.M. and Naef,F. (2018) Modulation of transcriptional burst frequency by histone acetylation. *Proc. Natl. Acad. Sci. U.S.A.*, **115**, 7153–7158.
73. Kebede,A.F., Nieborak,A., Shahidian,L.Z., Le Gras,S., Richter,F., Gomez,D.A., Baltissen,M.P., Meszaros,G., Magliarelli,H.F., Taudt,A. *et al.* (2017) Histone propionylation is a mark of active chromatin. *Nat. Struct. Mol. Biol.*, **24**, 1048–1056.
74. Miotto,B. and Struhl,K. (2010) HBO1 histone acetylase activity is essential for DNA replication licensing and inhibited by Geminin. *Mol. Cell*, **37**, 57–66.